

Merger of compact stars in the two families scenario

(based on: *Astrophys.J.* 852 (2018) no.2, L32; *Astrophys.J.* 846 (2017) no.2, 163; *Eur.Phys.J.* A52 (2016) no.2, 41; *Eur.Phys.J.* A52 (2016) no.2, 40)

Giuseppe Pagliara

Dipartimento di Fisica e Scienze della Terra, Università di Ferrara
and INFN



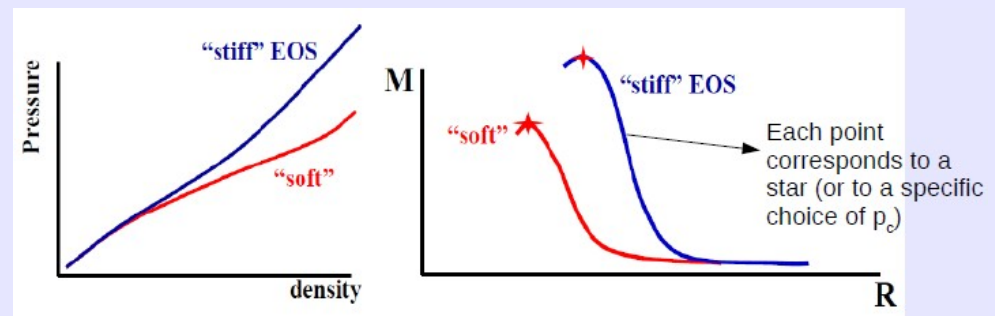
IWARA 2018 – Ollantaytambo - Peru'

Outline

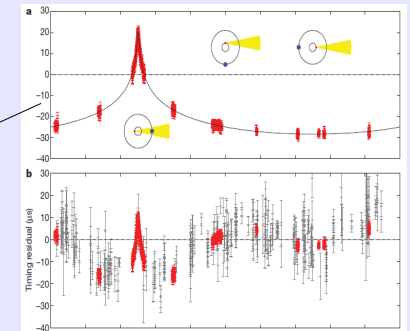
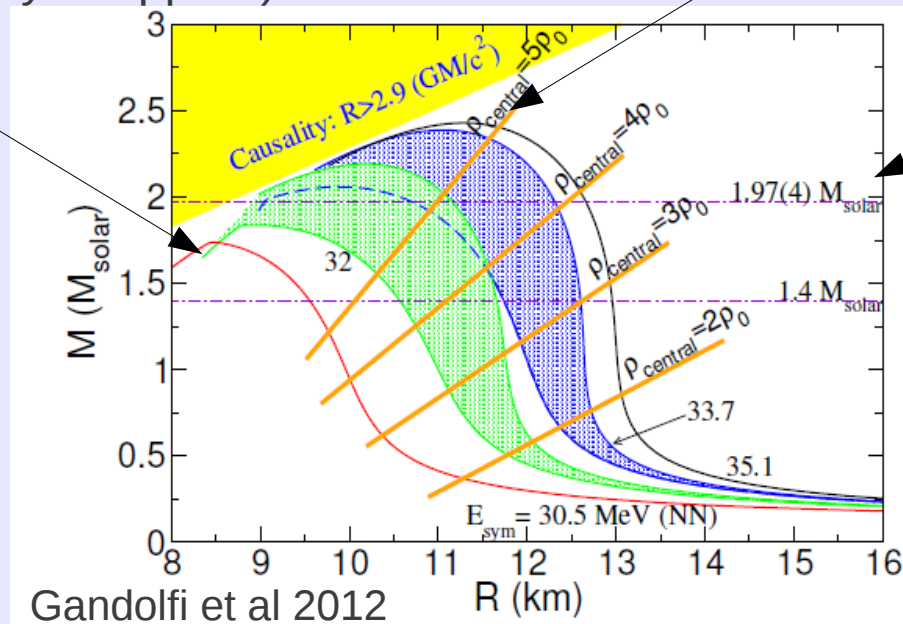
- Equation of state of dense matter: nucleonic matter, hadronic matter, strange quark matter (strangeon matter see Xu's talk)
- Structure of compact stars
- Merger of compact stars in the era of multi-messenger astronomy
- Need of two families of compact stars? Signatures
- Conclusions

The (unknown) equation of state of dense matter: soft, stiff or “both”?

Soft: small maximum mass – compact configurations, large central densities, large central baryon chemical potential (which could reach 1.5 GeV, hyperons and deltas resonances likely to appear)



Stiff: high maximum mass – less compact configurations, small central densities, small central baryon chemical potential



Strongest and reliable constraint from **Shapiro delay: maximum mass of at least $2M_{\text{sun}}$**

Example of two radii measurements

THE NEAREST MILLISECOND PULSAR REVISITED WITH *XMM-NEWTON*: IMPROVED MASS-RADIUS CONSTRAINTS FOR PSR J0437-4715

SLAVKO BOGDANOV

Columbia Astrophysics Laboratory, Columbia University, 550 West 120th Street, New York, NY 10027, USA; slavko@astro.columbia.edu
and

Department of Physics, McGill University, 3600 University Street, Montreal, QC H3A 2T8, Canada

Received 2012 July 17; accepted 2012 November 17; published 2012 December 19

ABSTRACT

I present an analysis of the deepest X-ray exposure of a radio millisecond pulsar (MSP) to date, an *X-ray Multi Mirror-Newton* European Photon Imaging Camera spectroscopic and timing observation of the nearest known MSP, PSR J0437-4715. The timing data clearly reveal a secondary broad X-ray pulse offset from the main pulse by ~ 0.55 in rotational phase. In the context of a model of surface thermal emission from the hot polar caps of the neutron star, this can be plausibly explained by a magnetic dipole field that is significantly displaced from the stellar center. Such an offset, if commonplace in MSPs, has important implications for studies of the pulsar population, high energy pulsed emission, and the pulsar contribution to cosmic-ray positrons. The continuum emission shows evidence for at least three thermal components, with the hottest radiation most likely originating from the hot magnetic polar caps and the cooler emission from the bulk of the surface. I present pulse phase-resolved X-ray spectroscopy of PSR J0437-4715, which for the first time properly accounts for the system geometry of a radio pulsar. Such an approach is essential for unbiased measurements of the temperatures and emission areas of polar cap radiation from pulsars. Detailed modeling of the thermal pulses, including relativistic and atmospheric effects, provides a constraint on the redshift-corrected neutron star radius of $R > 11.1$ km (at 3σ conf.) for the current radio timing mass measurement of $1.76 M_{\odot}$. This limit favors “stiff” equations of state.

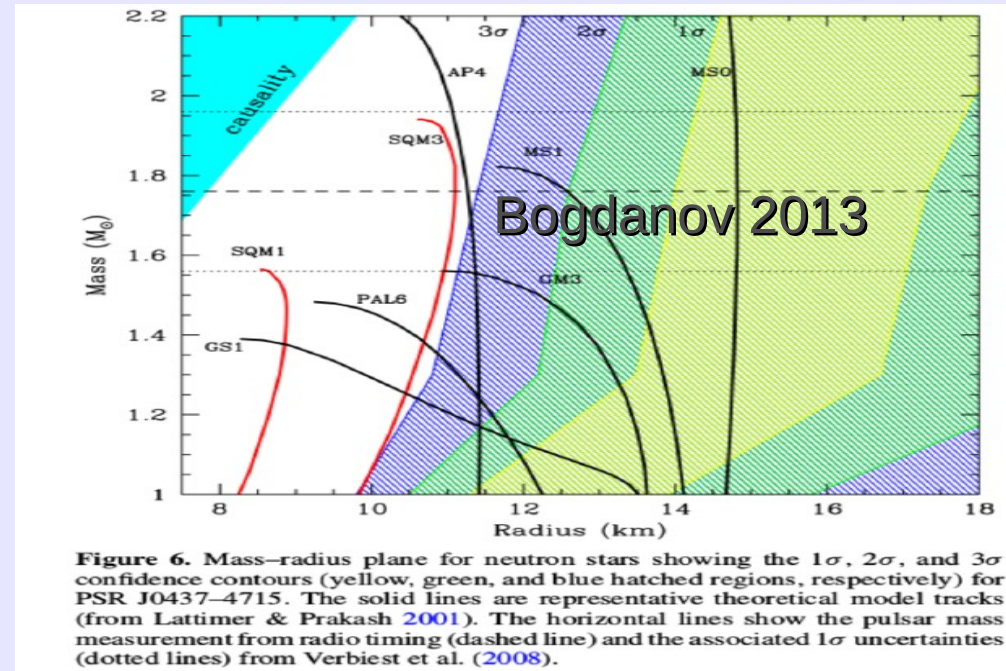


Figure 6. Mass-radius plane for neutron stars showing the 1σ , 2σ , and 3σ confidence contours (yellow, green, and blue hatched regions, respectively) for PSR J0437-4715. The solid lines are representative theoretical model tracks (from Lattimer & Prakash 2001). The horizontal lines show the pulsar mass measurement from radio timing (dashed line) and the associated 1σ uncertainties (dotted lines) from Verbiest et al. (2008).

NEUTRON STAR MASS-RADIUS CONSTRAINTS OF THE QUIESCENT LOW-MASS X-RAY BINARIES X7 AND X5 IN THE GLOBULAR CLUSTER 47 TUC

SLAVKO BOGDANOV¹, CRAIG O. HEINKE², FERYAL ÖZEL³, AND TOLGA GÜVER⁴

¹ Columbia Astrophysics Laboratory, Columbia University, 550 West 120th Street, New York, NY 10027, USA

² Department of Physics, University of Alberta, CCIS 4-183, Edmonton AB T6G 2E1, Canada

³ Department of Astronomy, University of Arizona, 933 North Cherry Avenue, Tucson, AZ 85721, USA

⁴ Istanbul University, Science Faculty, Department of Astronomy and Space Sciences, Beyazıt, 34119, Istanbul, Turkey

Received 2016 March 4; revised 2016 August 9; accepted 2016 August 18; published 2016 November 7

ABSTRACT

We present *Chandra*/ACIS-S subarray observations of the quiescent neutron star (NS) low-mass X-ray binaries X7 and X5 in the globular cluster 47 Tuc. The large reduction in photon pile-up compared to previous deep exposures enables a substantial improvement in the spectroscopic determination of the NS radius and mass of these NSs. Modeling the thermal emission from the NS surface with a non-magnetized hydrogen atmosphere and accounting for numerous sources of uncertainties, we obtain for the NS in X7 a radius of $R = 11.1^{+0.8}_{-0.7}$ km for an assumed stellar mass of $M = 1.4 M_{\odot}$ (68% confidence level). We argue, based on astrophysical grounds, that the presence of a He atmosphere is unlikely for this source. Due to the excision of data affected by eclipses and variable absorption, the quiescent low-mass X-ray binary X5 provides less stringent constraints, leading to a radius of $R = 9.6^{+0.9}_{-1.1}$ km, assuming a hydrogen atmosphere and a mass of $M = 1.4 M_{\odot}$. When combined with all existing spectroscopic radius measurements from other quiescent low-mass X-ray binaries and Type I X-ray bursts, these measurements strongly favor radii in the 9.9–11.2 km range for a $\sim 1.5 M_{\odot}$ NS and point to a dense matter equation of state that is somewhat softer than the nucleonic ones that are consistent with laboratory experiments at low densities.

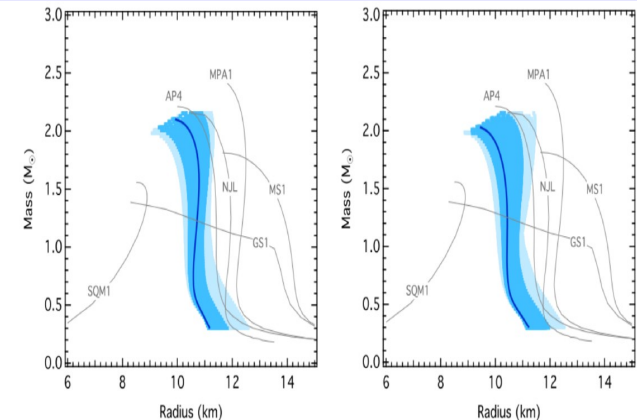
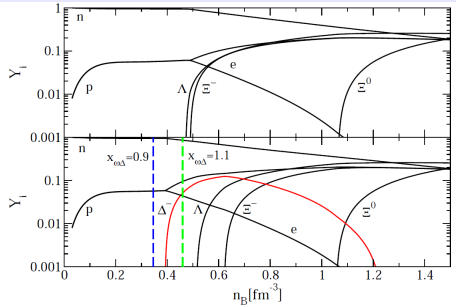


Figure 10. Mass-radius relation (solid blue curve) corresponding to the most likely triplet of pressures that agrees with the current neutron star data. These include the X5 and X7 radius measurements shown in this work, as well as the neutron star radius measurements for the 12 neutron stars included in Özel et al. (2016), the low-energy nucleon-nucleon scattering data, and the requirement that the EoS allow for a $M > 1.97 M_{\odot}$ neutron star. The ranges of mass-radius relations corresponding to the regions of the P_1, P_2, P_3 parameter space in which the likelihood is within $e^{-1/2}$ and e^{-1} of its highest value are shown in dark and light blue bands, respectively. The results for flat priors in P_1, P_2 , and P_3 (top panel) and for flat priors on the logarithms of these pressures (bottom panel) are shown.

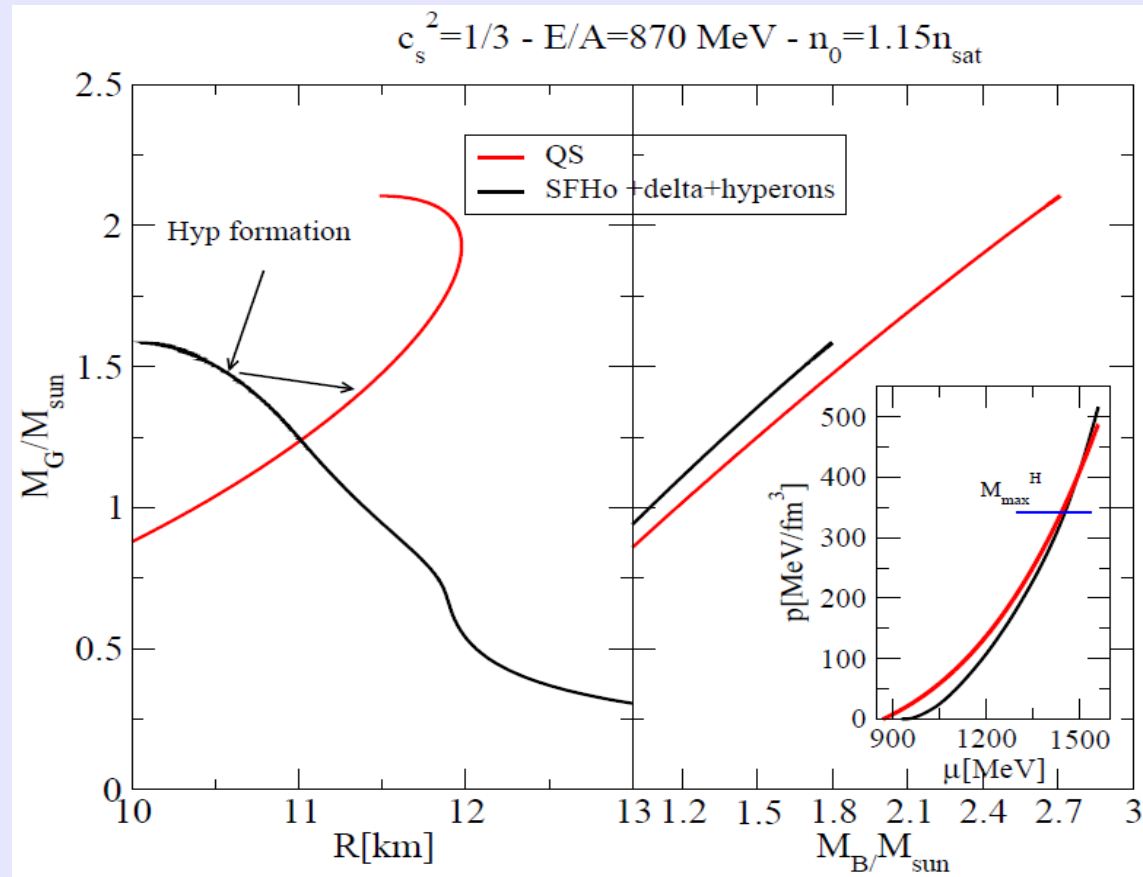
Different stellar objects, different techniques... still, **some indication of large stars (>12 km) and small stars (<11km)**

Two families of compact stars?

(exercise with constant speed of sound quark EoS, Dondi et al 2016)



RMF model for hadronic matter



Three parameters:
Speed of sound, energy density and baryon density at pressure=0

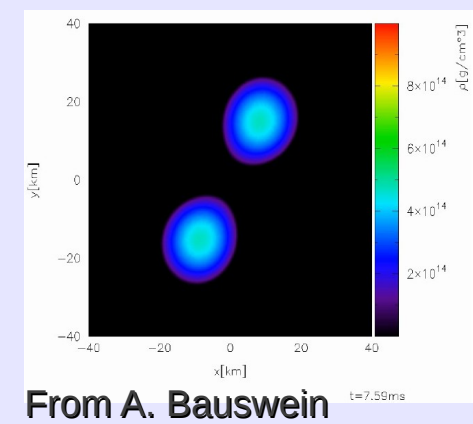
$$p = c_s^2(e - e_0)$$

$$k = \frac{e_0 c_s^2}{1 + c_s^2}$$

$$p = k((n/n_0)^{1+c_s^2} - 1)$$

Hadronic stars would fulfill the small radii limits while strange stars would fulfill the large masses limits. Note: at fixed baryon mass, strange stars could be energetically convenient even if the radius is larger than the corresponding hadronic star configuration.

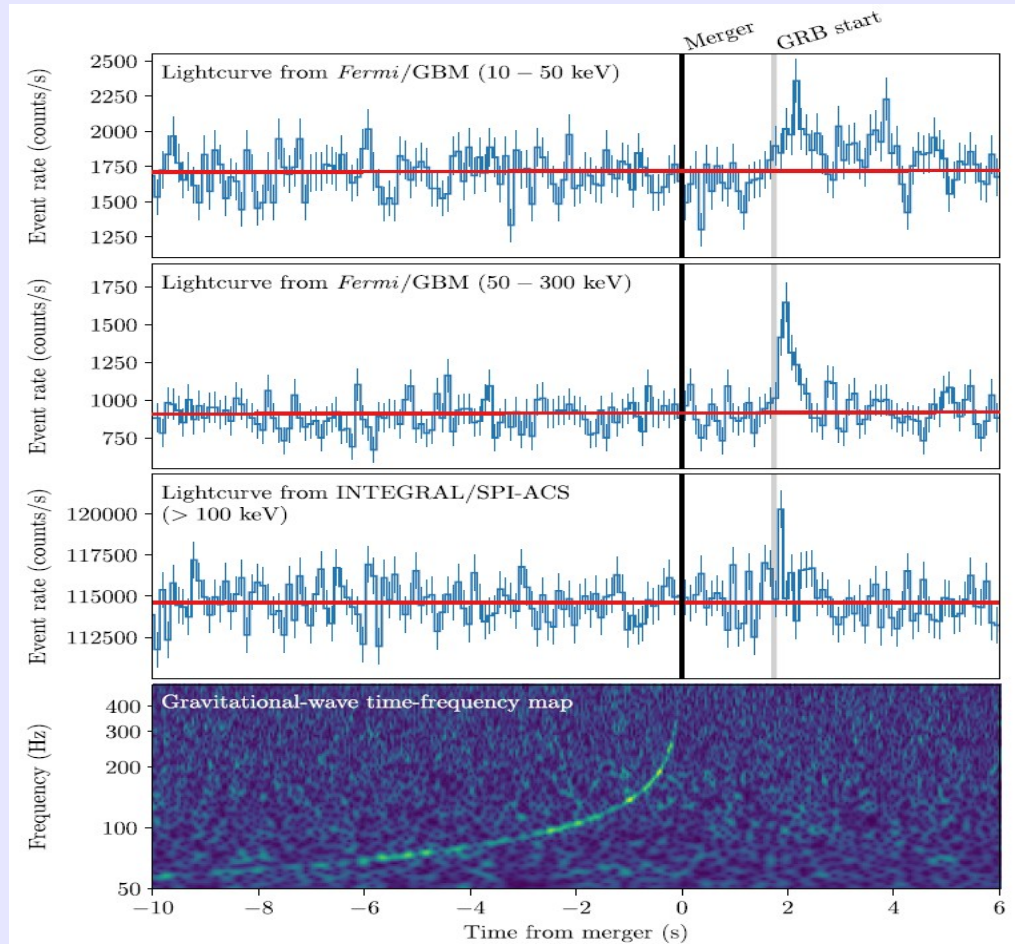
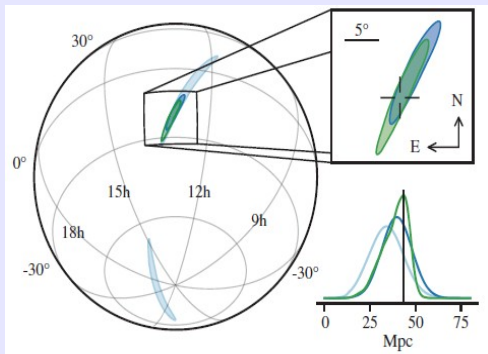
August 2017: The first (multimessenger) detection of a neutron star – neutron star merger



1) Gravitational waves from the inspiral phase seen by LIGO&VIRGO

2) Prompt short gamma-ray-burst seen by FERMI&INTEGRAL delayed by about 2 sec and lasting about 2sec. Very low luminosity as compared to standard sGRBs: 10^{47} erg/sec

3) Localization of the source (the host galaxy) and estimate of the distance: 40Mpc



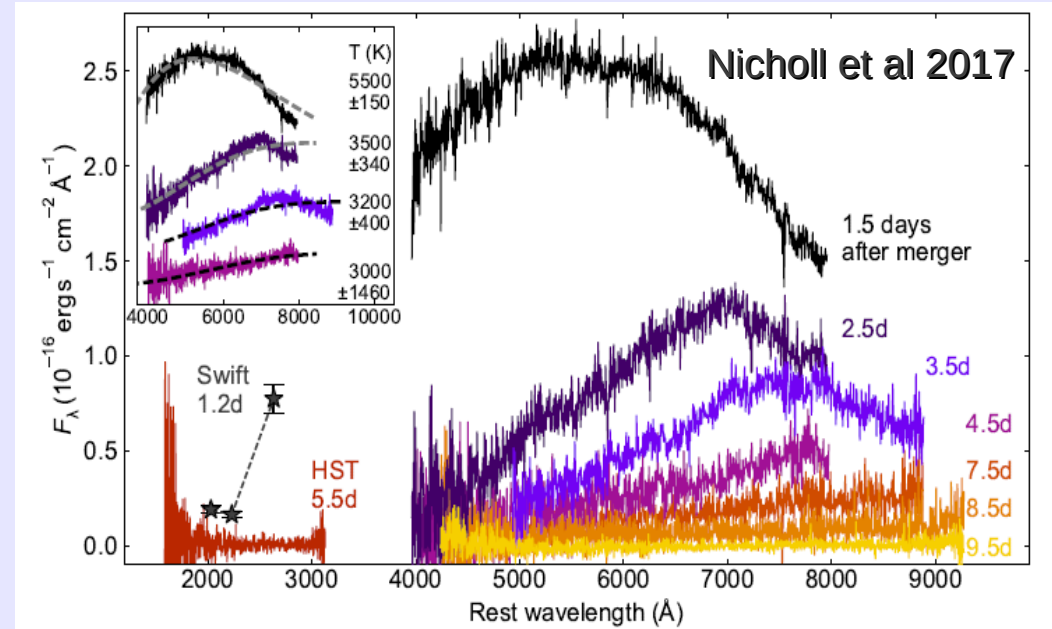
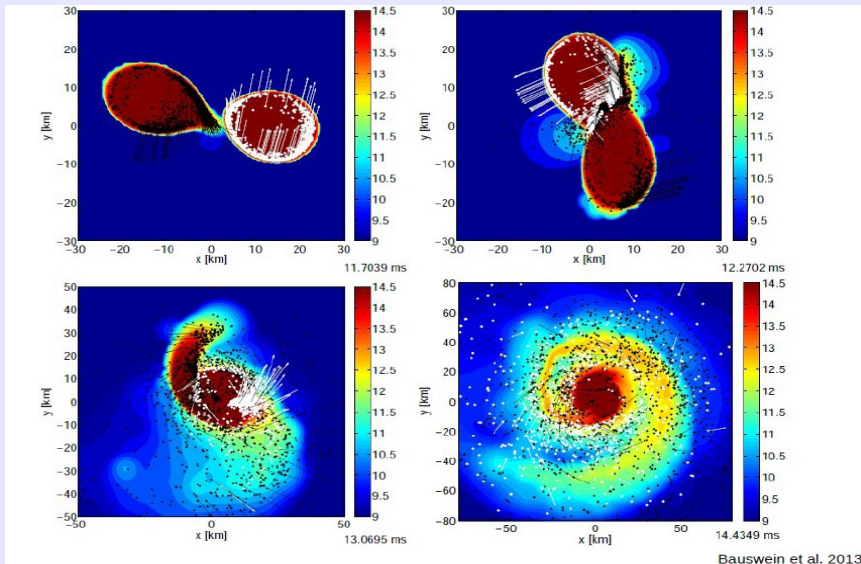
Abbott et al, APJL 2017.

The subsequent kilonova

The merger of two neutron stars leads to the ejection of neutron rich material.

Fitting the spectra:

- 1) amount of ejected material: few $10^{-2} M_{\text{sun}}$
- 2) speed of the expanding material: few $0.1c$
- 3) different components (red & blue kilonova):
 material ejected from tidal disruption
 shock heated material
 accretion disk wind



The kilonova signal is due to the radioactive decays of the heavy elements synthesized in the ejecta (similar to the a supernova which is powered by the decay of ^{56}Ni).

What do we learn from the measured GW signal:

The power and frequency of the GW signal during the inspiral phase depend on the chirp mass which in turn is related to the total mass.

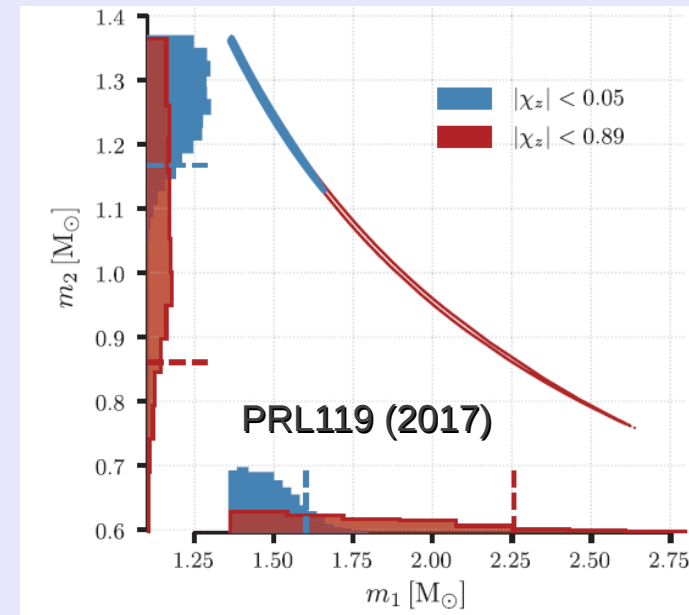
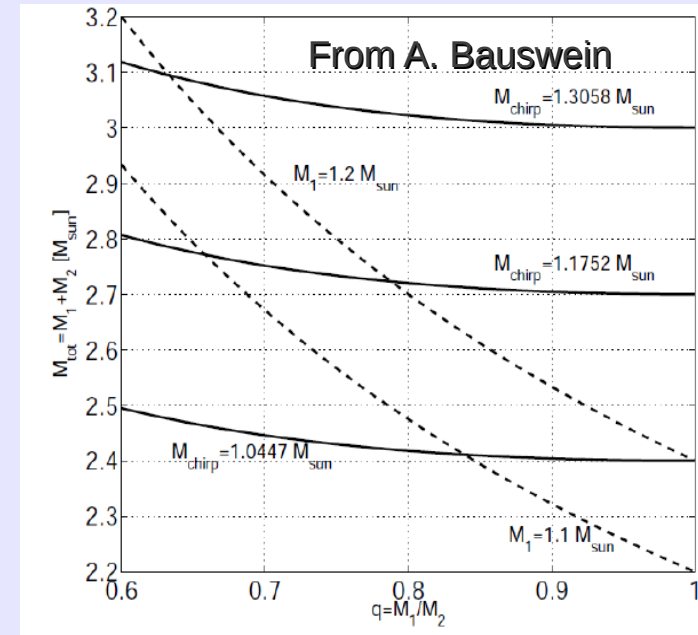
$$M_{\text{chirp}} = (M_1 M_2)^{3/5} (M_1 + M_2)^{-1/5}$$

Measurement: $M_{\text{chirp}} = 1.188 M_{\text{sun}}$ which leads to a total mass

$$M_{\text{tot}} = M_1 + M_2 = 2.74^{+0.04}_{-0.02} M_{\odot}$$

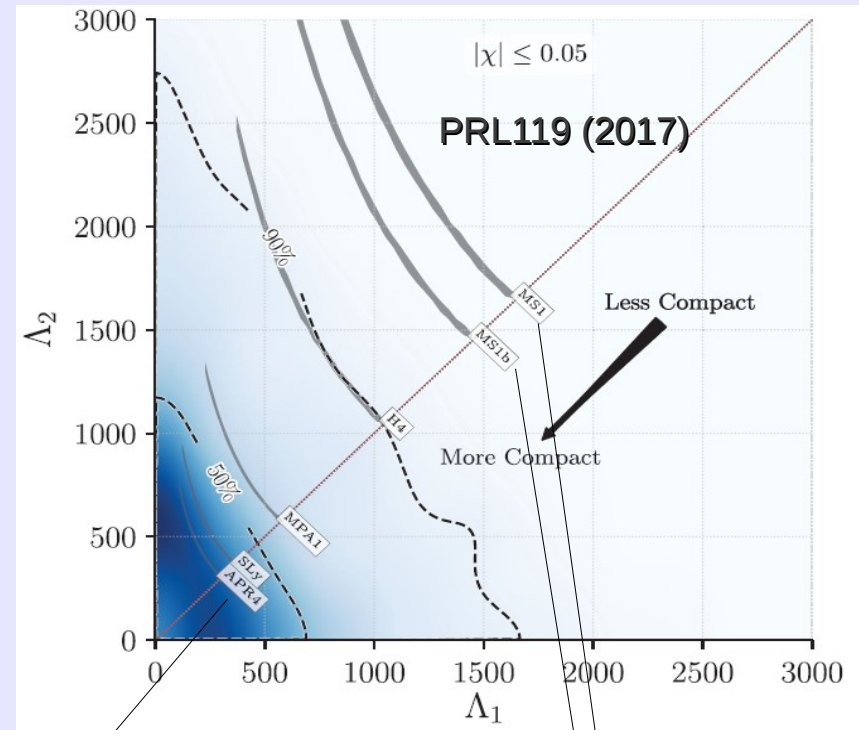
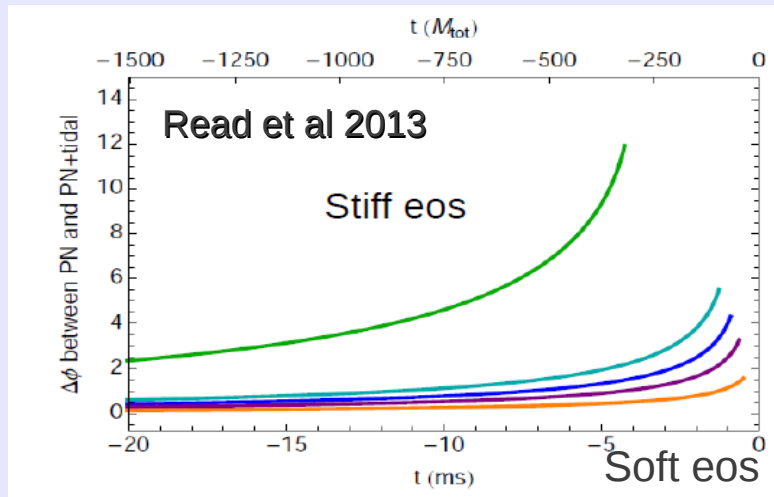
Indications of an asymmetric system: $M_1 \sim 1.36 - 1.6 M_{\text{sun}}$
 $M_2 \sim 1.17 - 1.36 M_{\text{sun}}$

Values consistent with the distribution of masses in binary systems. Consistent with the hyp. that the two compact stars are both neutron stars (BH -NS system very unlikely)



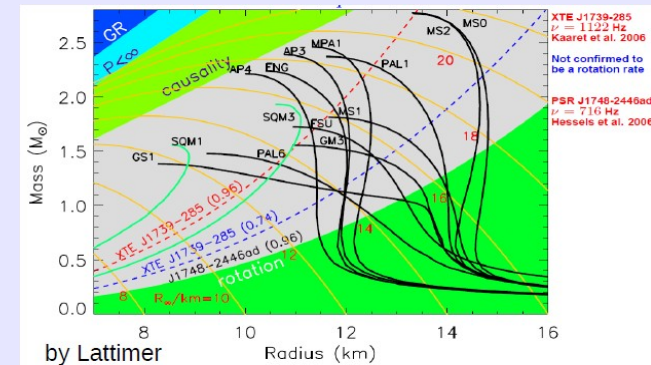
Compactness constraints

The deviations from point-like GW sources depend on the tidal deformability Λ : the phase departure depend on the compactness of the stars and thus on the equation of state. The stiffer the EoS the larger the radius, the larger the deviation.



Ruled out, ingredients: just nucleons, no strangeness. Large radii.

Sly and APR4: again just nucleons, but consistent with the astro-data. Are they consistent with (hyper)nuclear physics ??



Example: Sly equation of state (Douchin&Hansel 2001)

dof: nucleons and leptons, Skyrme type interactions. No hyperons , no deltas included.

EOS	M [M_{\odot}]	R [km]	n_c [fm $^{-3}$]	ρ_c [10^{15} g/cm 3]	P_c [10^{36} dyn/cm 2]	A [10^{57}]	z_{surf}	E_{bind} [10^{53} erg]	I [10^{45} g cm 2]
SLy	2.05	9.99	1.21	2.86	1.38	2.91	0.594	6.79	1.91
FPS	1.80	9.27	1.46	3.40	1.37	2.52	0.531	5.37	1.36

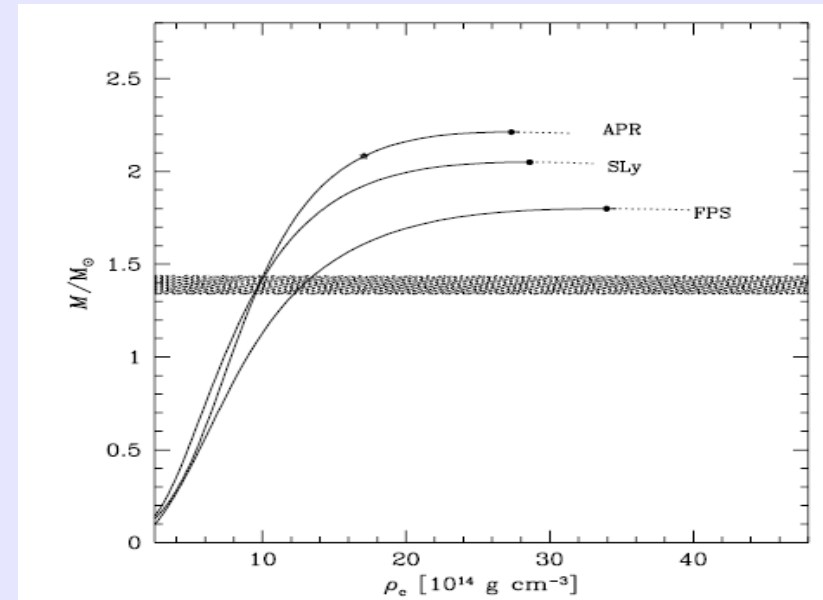


Fig. 4. Gravitational mass M versus central density ρ_c , for the SLy, FPS, and APR EOS of dense matter. Maximum on the mass-central density curves is indicated by a filled circle. On the APR curve, configurations to the right of the asterisk contain a central core with $v_{sound} > c$. Configurations to the right of the maxima are unstable with respect to small radial perturbations, and are denoted by a dotted line. The shaded band corresponds to the range of precisely measured masses of binary radio pulsars.

Calculations performed much before the discovery of the $2M_{sun}$ stars. At the maximum mass densities close to 10 times saturation density.

In general : soft nucleonic equations of state predict large densities. Heavy baryons must be taken into account at such high densities!!

Constraints from the amount of matter ejected

TABLE I. Equations of state employed, the maximum mass for cold spherical neutron stars, M_{\max} , in units of the solar mass, the radius, R_M , and the dimensionless tidal deformability Λ_M of spherical neutron stars of gravitational mass $M = 1.20, 1.30, 1.40$, and $1.50M_{\odot}$. R_M is listed in units of km. The last five data show the binary tidal deformability for $\eta = 0.250, 0.248, 0.246, 0.244$, and 0.242 with $\mathcal{M} = 1.19M_{\odot}$.

EOS	M_{\max}	$R_{1.20}$	$R_{1.30}$	$R_{1.40}$	$R_{1.50}$	$\Lambda_{1.20}$	$\Lambda_{1.30}$	$\Lambda_{1.40}$	$\Lambda_{1.50}$	Λ
SFH _o	2.06	11.96	11.93	11.88	11.83	864	533	332	208	388, 387, 387, 386, 385
DD2	2.42	13.14	13.18	13.21	13.24	1622	1053	696	467	797, 788, 780, 772, 764

TABLE II. Merger remnants and properties of dynamical ejecta for two finite-temperature neutron-star EOS, SFH_o and DD2 and for the cases with different mass. The quantities for the remnants are determined at ≈ 30 ms after the onset of merger. HMNS, BH, and MNS denote hypermassive neutron star, black hole, and massive neutron star, respectively. The torus mass for the DD2 EOS is determined from the mass located outside the central region of MNS with density $\rho \leq 10^{13}$ g/cm³. The values of mass are shown in units of M_{\odot} . The BH spin means the dimensionless spin of the remnant black hole. Y_e and \bar{v}_{ej} are the average value of the electron fraction, Y_e , and average velocity of the dynamical ejecta, respectively. We note that Y_e is broadly distributed between ~ 0.05 and ~ 0.5 , irrespective of the models (see Refs. [34, 35]).

EOS	m_1 & m_2	m_2/m_1	Remnant	BH mass	BH spin	Torus mass	M_{ej}	Y_e	\bar{v}_{ej}/c
SFH _o	1.35, 1.35	1.00	HMNS \rightarrow BH	2.59	0.69	0.05	0.011	0.31	0.22
SFH _o	1.37, 1.33	0.97	HMNS \rightarrow BH	2.59	0.70	0.06	0.008	0.30	0.21
SFH _o	1.40, 1.30	0.93	HMNS \rightarrow BH	2.58	0.67	0.09	0.006	0.27	0.20
SFH _o	1.45, 1.25	0.86	HMNS \rightarrow BH	2.58	0.69	0.12	0.011	0.18	0.24
SFH _o	1.55, 1.25	0.81	HMNS \rightarrow BH	2.69	0.76	0.07	0.016	0.13	0.25
SFH _o	1.65, 1.25	0.76	BH	2.76	0.77	0.09	0.007	0.16	0.23
DD2	1.35, 1.35	1.00	MNS	—	—	0.23	0.002	0.30	0.16
DD2	1.40, 1.30	0.93	MNS	—	—	0.23	0.003	0.26	0.18
DD2	1.45, 1.25	0.86	MNS	—	—	0.30	0.005	0.20	0.19
DD2	1.40, 1.40	1.00	MNS	—	—	0.17	0.002	0.31	0.16

Comparison between a soft and stiff equation of state (Shibata et al 2017)

Computations of mass ejected not yet completely under control: for instance the neutrino transport is modeled by simple leakage schemes.

THE ELECTROMAGNETIC COUNTERPART OF THE BINARY NEUTRON STAR MERGER LIGO/VIRGO GW170817. III. OPTICAL AND UV SPECTRA OF A BLUE KILONOVA FROM FAST POLAR EJECTA

M. NICHOLL¹, E. BERGER¹, D. KASEN^{2,3}, B. D. METZGER⁴, J. ELIAS⁵, C. BRICEÑO⁶, K. D. ALEXANDER¹, P. K. BLANCHARD¹, R. CHORNOCK⁷, P. S. COWPERTHWAIT¹, T. EFTEKHARI¹, W. FONG⁸, R. MARGUTTI⁸, V. A. VILLAR¹, P. K. G. WILLIAMS¹, W. BROWN¹, J. ANNIS⁹, A. BAHRAMIAN¹⁰, D. BROUT¹¹, D. A. BROWN¹², H.-Y. CHEN¹³, J. C. CLEMENS¹⁴, E. DENNIHY¹⁴, B. DUNLAP¹⁴, D. E. HOLZ^{15,13,16,17}, E. MARCHESINI^{18,19,20,21,22}, F. MASSARO^{20,21,23}, N. MOSKOVITZ²⁴, I. PELISOLI^{25,26}, A. REST^{27,28}, F. RICCI^{29,1}, M. SAKO¹¹, M. SOARES-SANTOS^{9,30}, J. STRADER¹⁰

ABSTRACT

We present optical and ultraviolet spectra of the first electromagnetic counterpart to a gravitational wave (GW) source, the binary neutron star merger GW170817. Spectra were obtained nightly between 1.5 and 9.5 days post-merger, using the SOAR and Magellan telescopes; the UV spectrum was obtained with the *Hubble Space Telescope* at 5.5 days. Our data reveal a rapidly-fading blue component ($T \approx 5500$ K at 1.5 days) that quickly reddens; spectra later than $\gtrsim 4.5$ days peak beyond the optical regime. The spectra are mostly featureless, although we identify a possible weak emission line at ~ 7900 Å at $t \lesssim 4.5$ days. The colours, rapid evolution and featureless spectrum are consistent with a “blue” kilonova from polar ejecta comprised mainly of light r -process nuclei with atomic mass number $A \lesssim 140$. This indicates a sight-line within $\theta_{\text{obs}} \lesssim 45^\circ$ of the orbital axis. Comparison to models suggests $\sim 0.03 M_{\odot}$ of blue ejecta, with a velocity of $\sim 0.3c$. The required lanthanide fraction is $\sim 10^{-4}$, but this drops to $< 10^{-5}$ in the outermost ejecta. The large velocities point to a dynamical origin, rather than a disk wind, for this blue component, suggesting that both binary constituents are neutron stars (as opposed to a binary consisting of a neutron star and a black hole). For dynamical ejecta, the high mass favors a small neutron star radius of $\lesssim 12$ km. This mass also supports the idea that neutron star mergers are a major contributor to r -process nucleosynthesis.

Average tidal deformability

$$\tilde{\Lambda} = \frac{16}{13} \left[\frac{(M_A + 12M_B)M_A^4 \tilde{\Lambda}_A}{(M_A + M_B)^5} + (A \leftrightarrow B) \right]$$

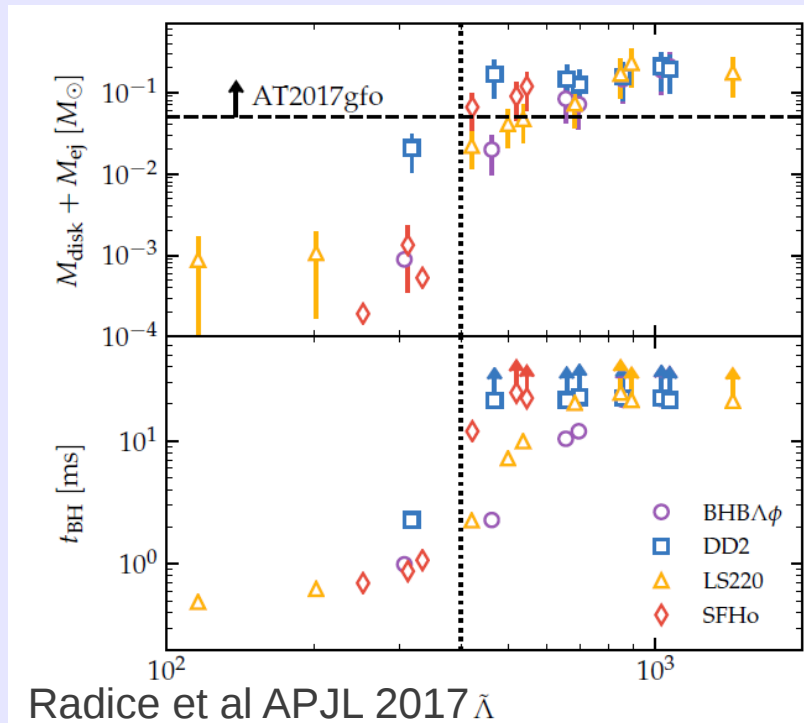
From numerical simulations: an empirical relation between the average tidal deformability and the sum of the mass ejected and the mass of the accreting disk.

Estimate of the lower limit on the average tidal deformability ~ 400

Use of chiral effective theory results for subsaturation densities and pQCD calculations at (very) high densities and interpolate between them with piecewise polytropes

$2M_{\text{sun}}$ limit and constraints on the tidal deformability obtained with GW170817 : $400 < \Lambda < 800$ for a $1.4 M_{\text{sun}}$.

Its radius **$12.2\text{km} < R_{1.4} < 13.4\text{km}$**
(tension with small radii measurements)



Radice et al APJL 2017 $\tilde{\Lambda}$

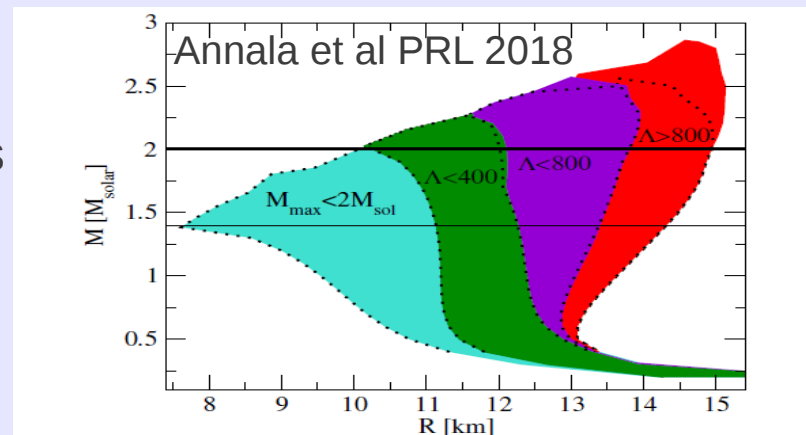


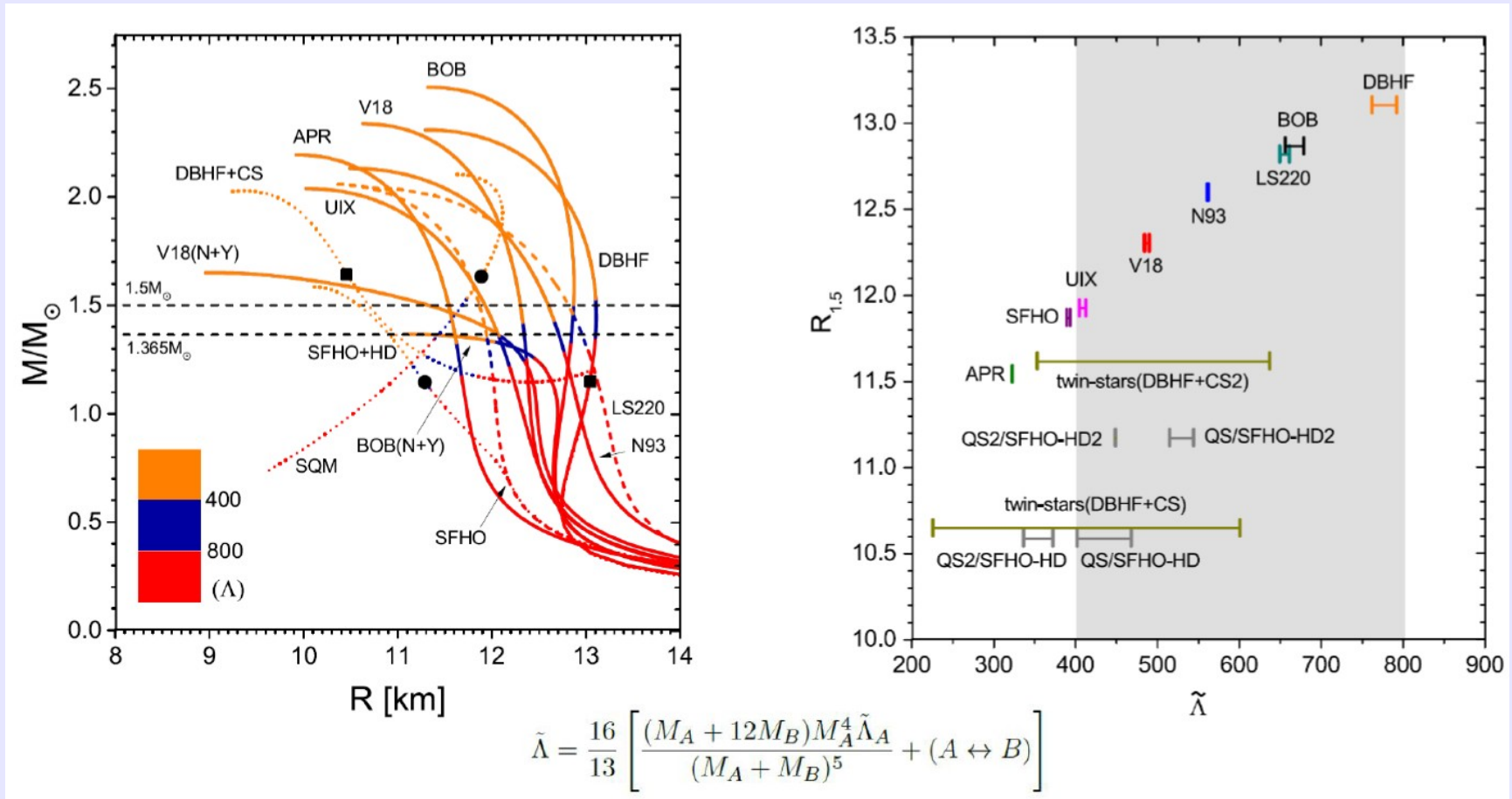
FIG. 1: The mass-radius clouds corresponding to our EoSs. The cyan area corresponds to EoSs that cannot support a $2M_{\odot}$ star, while the rest denote EoSs that fulfill this requirement and in addition have $\Lambda(1.4M_{\odot}) < 400$ (green), $400 < \Lambda(1.4M_{\odot}) < 800$ (violet), or $\Lambda(1.4M_{\odot}) > 800$ (red), so that the red region is excluded by the LIGO/Virgo measurement at 90% credence. This color coding is used in all of our figures. The dotted black lines denote the result that would have been obtained with bitropic interpolation only.

GW170817 within the two families scenario

- Three possible merger processes: double hadronic stars system, hadronic star - quark star (mixed), double quark stars system
 - a) The total mass of GW170817 is larger than the threshold mass above which a prompt collapse is obtained in the case of a double hadronic stars system ($M_{\text{threshold}} \sim 2.5 M_{\text{sun}}$). The electromagnetic counterpart excludes the occurrence of a prompt collapse for GW170817 thus it cannot be a double hadronic stars system.
 - b) It cannot be due to a double quark stars system due the large amount of hadronic matter ejected from the merger (in turn this rules out the possibility that all compact stars are quark stars, caveat: evaporation of quark matter droplets?)
 - c) GW170817 is due, within the two families scenario, to the **merger of a mixed system** (similarly, for the twin stars scenario to be discussed by D. Blaschke, hybrid star – hadronic star)

Relation between average tidal deformability and radii:

(Burgio et al. ApJ 2018)



While for the standard one family scenario, a tidal deformability larger than 400 implies a radius larger than about 12km, within the two families scenario (and the twin stars scenario) it is possible to fulfill the constraints on the tidal deformability from GW170817 and to obtain at the same time radii smaller than about 11km (thus closer to some observational analyses on radii). This is due to the large difference in radii of the two components of the mixed binary system. Mass ejected? Difficult to estimate, need of hydro-simulations with two distinct fluids.

Predictions

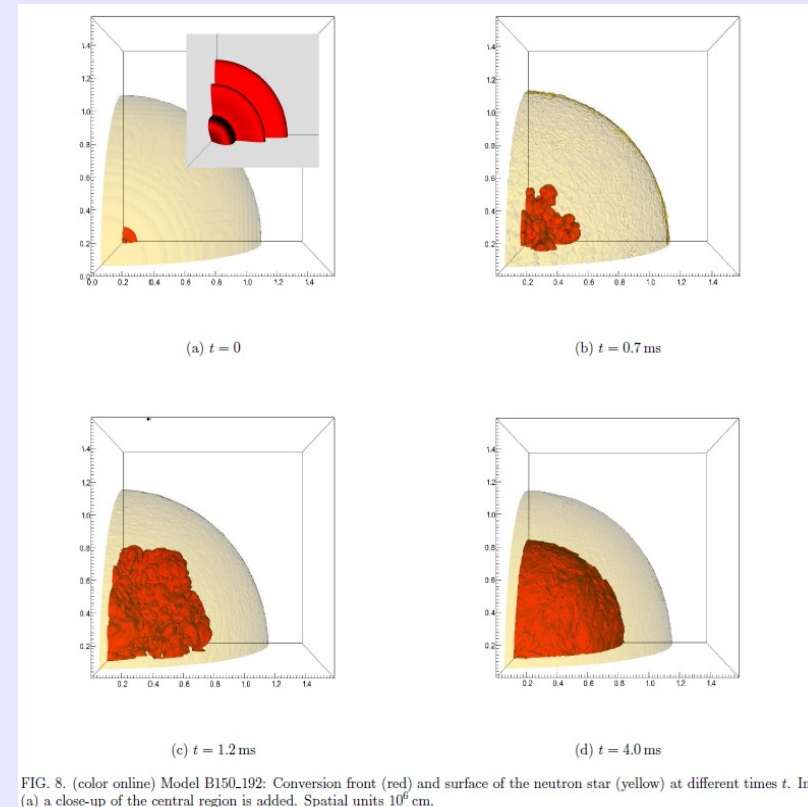
key points of the two families scenario:

- 1) A merger would always produce at some stage a strange star (stable or unstable) but for the case of the prompt collapse
- 2) In the cases of prompt collapse, the remnant collapses within $t_c \sim \text{few ms}$ which is comparable with the time needed for the turbulent conversion of the hadronic star, t_{turb} (again few ms, Drago et al 2015)
- 3) In the cases of prompt collapse the relevant M_{max} is not the maximum mass of strange stars but the maximum mass of hadronic stars which is in our scenario of the order of $1.5 - 1.6 M_{\text{sun}}$

We expect therefore to have a large number of cases in which the prompt collapse occurs.

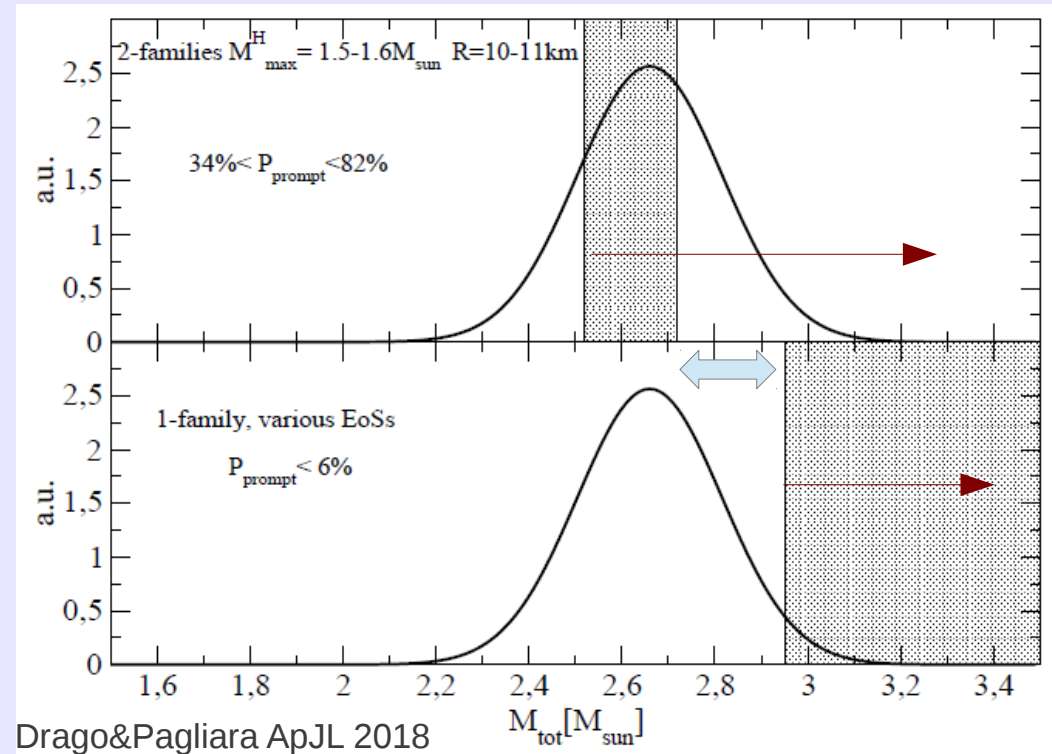
Conversion of a cold, non-rotating hadronic star

(Pagliara et al 2013)



Mass threshold for prompt collapse

By using the binary mass distribution (from Kiziltan 2013) we can calculate the probabilities of prompt collapses in the two families scenario and in the one family scenario.



In the two families scenario, if the two stars are both hadronic stars, it is very easy to obtain a prompt collapse.

The possibility of mixed systems, a quark star and a hadronic star, could lead to a non-monotonic behavior of the threshold mass as a function of the total mass (same total mass could lead to a prompt collapse or to a hypermassive/supramassive remnant).

If post-merger signal will be detected:

The GW frequency of the leading oscillation mode of the remnant as a function of the total mass of the binary: jump in correspondence of the threshold mass of the HS-HS system

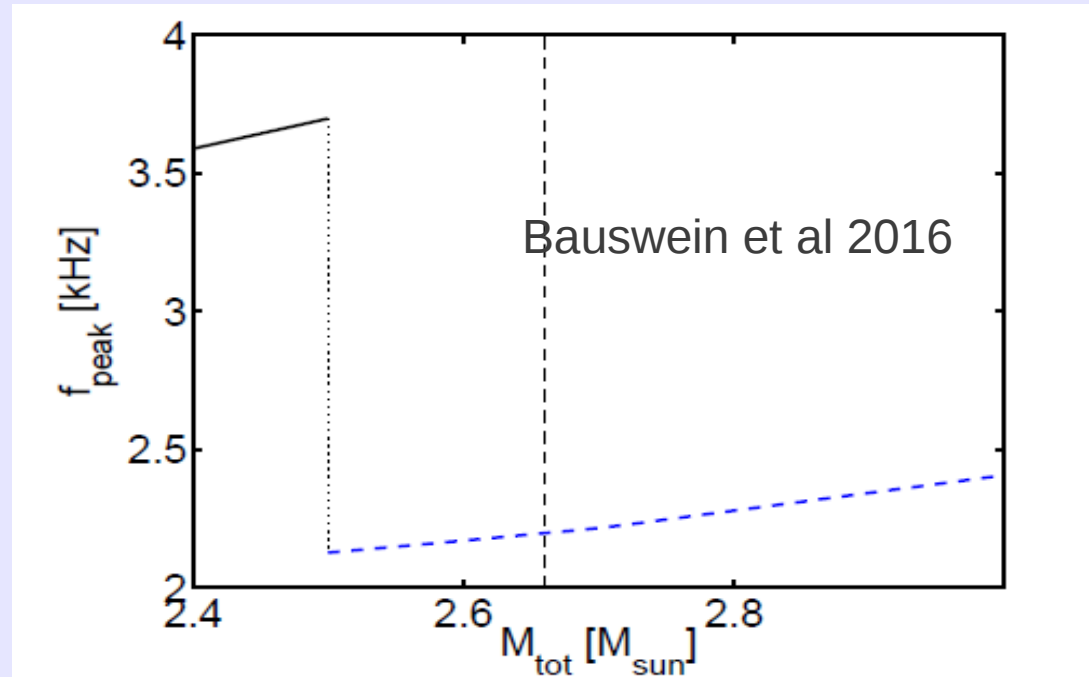


Fig. 17. Dominant postmerger GW frequency f_{peak} as a function of the total binary mass for symmetric mergers with a two-family scenario [46]. For low binary masses the merger remnant is composed of hadronic matter (black curve), whereas higher binary masses lead to the formation of a strange matter remnant with a lower peak frequency (dashed blue curve). The vertical dashed line marks a lower limit on the binary mass which is expected to yield a remnant that is stable against gravitational collapse (see text).

Possible types of mergers in the two-families scenario

- HS-HS

- For $M_{\text{tot}} > M_{\text{th}} \sim 2.48 M_{\text{S}}$ there is direct collapse to a BH
- For $M_{\text{tot}} < M_{\text{th}} \sim 2.48 M_{\text{S}}$ sGRB via the protomagnetar scheme
 - Possibility of extended emission and quasi-plateau
 - Large value of mass ejected by the shock, not very massive disk

- HS-QS

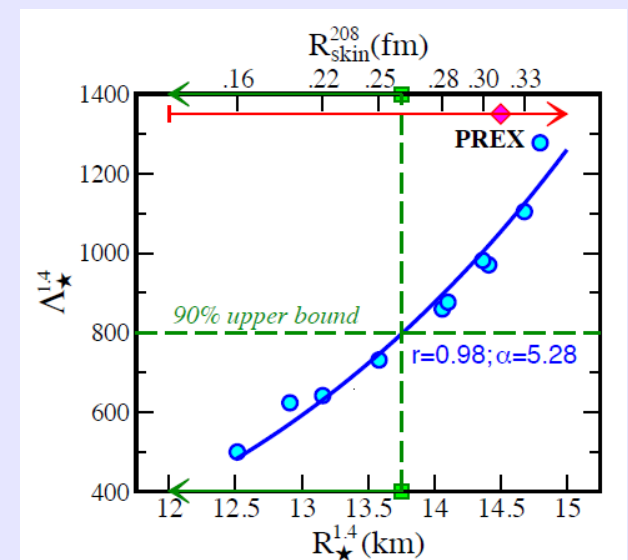
- For $M_{\text{tot}} > M_{\text{th}} \sim 3.1 M_{\text{S}}$ there is direct collapse to a BH
- For $2.6 M_{\text{S}} < M_{\text{tot}} < M_{\text{th}} \sim 3.1 M_{\text{S}}$ sGRB via BH and torus
 - No extended emission and no quasi plateau
 - Smaller value of mass ejected by the shock, massive disk
- For $M_{\text{tot}} < 2.6 M_{\text{S}}$ sGRB via the protomagnetar scheme
 - Possibility of extended emission and quasi-plateau
 - Smaller value of mass ejected by the shock, massive disk

- QS-QS

- For $M_{\text{tot}} > M_{\text{th}} \sim 3.1 M_{\text{S}}$ there is direct collapse to a BH
- For $M_{\text{tot}} < M_{\text{th}} \sim 3.1 M_{\text{S}}$ sGRB à la Haensel, Paczinski, Amsterdamski

Conclusions and future measurements

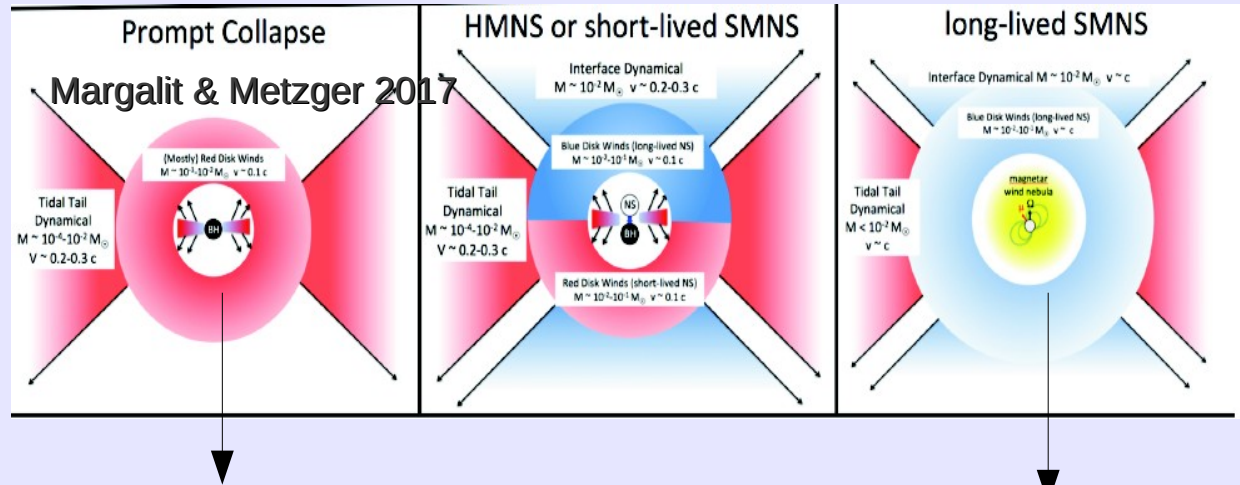
- With the expected rate of detection of merger events (~ 10 per year), confirm/rule out the two families scenario within a couple of years.
- Radii measurements (NICER):
 - $R_{1.4} > 13\text{km}$, one family of nucleonic stars (central density below the threshold of hyperons)
 - $11\text{ km} < R_{1.4} < 13\text{km}$, one family: hyperonic stars-hybrid stars (need of stiffening of the EoS to solve the hyperon puzzle)
 - $R_{1.4} < 11\text{km}$, two families scenario (or twin stars scenario)
- Neutron skin thickness:
if future measurements will indicate large values, a phase transition is likely to occur in compact stars (Fattoyev et al PRL2018)



Appendix

What do we learn from the measured EM signal:

- 1) At least one of the stars is a neutron star, most probably both (difficult to explain such small mass BHs)
- 2) From the three possible outcomes of a merger: Most probably a **hypermassive star** that collapsed to a BH within 1sec.



Stable until complete dissipation of differential rotation

Stable until complete dissipation of rigid rotation

Difficult to explain the shortGRB + small amount of mass ejected

To form a jet (needed for the short GRB) a black hole is needed (not clear however) + no evidence of long term energy injection

The merger of neutron stars represents a viable and maybe the most important mechanism for the nucleosynthesis of heavy elements via r-processes.

Constraining the equation of state: maximum mass

By using the hyp. that the remnant is not a supramassive star, three different papers lead to a maximum mass for cold and non-rotating star $M_{\max} \leq 2.2 M_{\text{sun}}$ (see also Margalit et al 2017)

Ruiz et al 2017:

$$M_{\text{NSNS}} \approx 2.74 \lesssim M_{\text{thresh}} \approx \alpha M_{\text{max}}^{\text{sph}}$$

$$M_{\text{NSNS}} \approx 2.74 \gtrsim M_{\text{max}}^{\text{sup}} \approx \beta M_{\text{max}}^{\text{sph}}$$

$$M_{\text{max}}^{\text{sph}} = 4.8 \left(\frac{2 \times 10^{14} \text{ gr/cm}^3}{\rho_m/c^2} \right)^{1/2} M_{\odot}$$

$$M_{\text{max}}^{\text{sup}} = 6.1 \left(\frac{2 \times 10^{14} \text{ gr/cm}^3}{\rho_m/c^2} \right)^{1/2} M_{\odot}$$

$$\beta \approx 1.27.$$

$$2.74/\alpha \lesssim M_{\text{max}}^{\text{sph}} \lesssim 2.74/\beta$$

(simple argument based on causality)

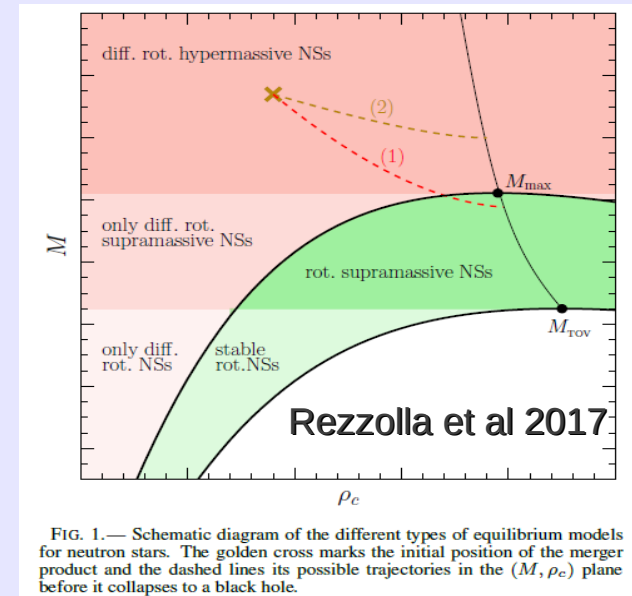


FIG. 1.— Schematic diagram of the different types of equilibrium models for neutron stars. The golden cross marks the initial position of the merger product and the dashed lines its possible trajectories in the (M, ρ_c) plane before it collapses to a black hole.

Ruling out very stiff equations of state!!



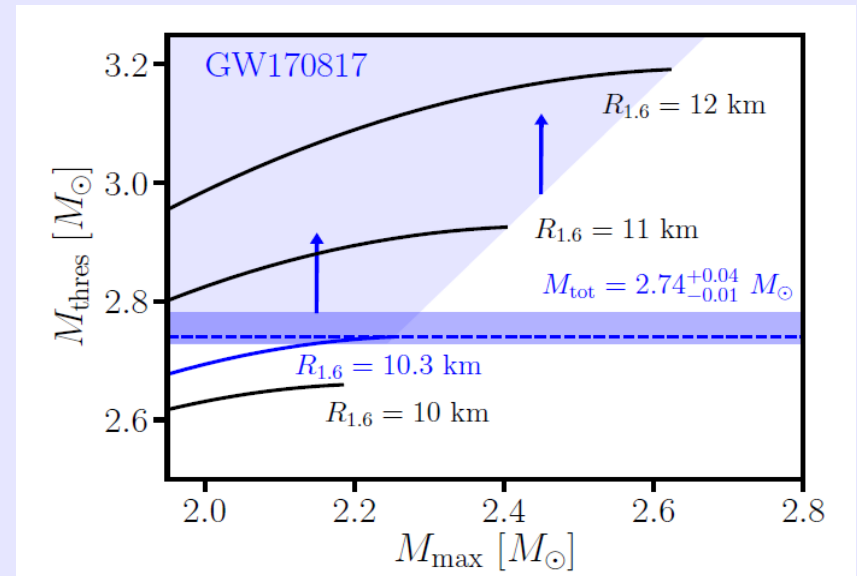
Constraining the equation of state: radii

Hyp: no prompt collapse in GW170817.
 Use of empirical relations between the maximum mass and the radius $R_{1.6}$ of the $1.6M_{\text{sun}}$ configuration found in numerical simulations of the merger.
 (Bauswein et al 2017)

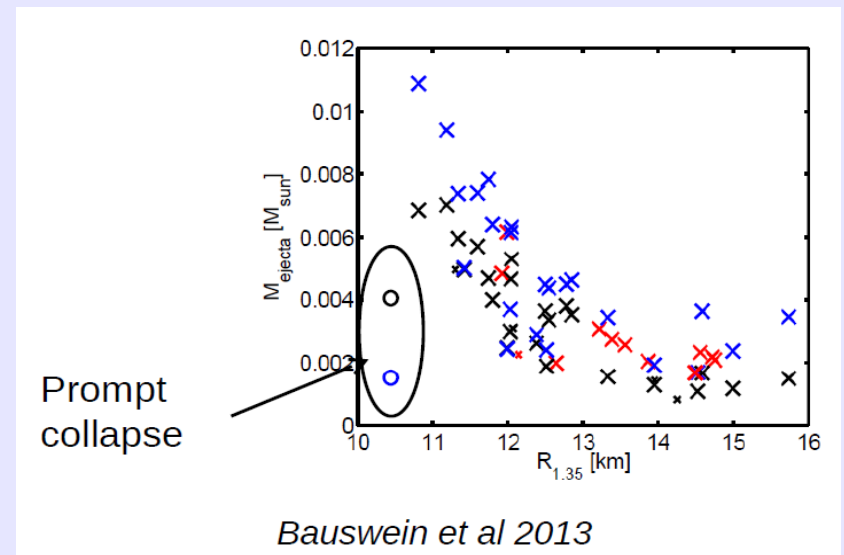
$$M_{\text{thres}} = \left(-3.606 \frac{GM_{\text{max}}}{c^2 R_{1.6}} + 2.38 \right) \cdot M_{\text{max}}$$

$$M_{\text{thres}} > M_{\text{tot}}^{\text{GW170817}} = 2.74^{+0.04}_{-0.01} M_{\odot}$$

Strong dependence of the mass ejected on the radius of the $1.35 M_{\text{sun}}$ configuration.
 The estimate of the ejected mass obtained from the kilonova would suggest radii smaller than about 11km!!.



$R_{1.6}$ larger than about 10.3km



First scenario: $11\text{km} < R_{1.4} < 13\text{km}$

Hybrid stars

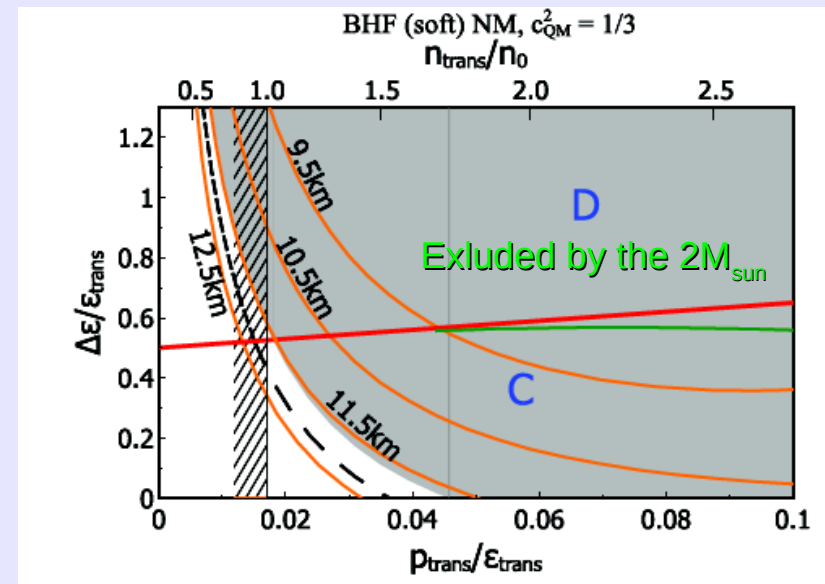
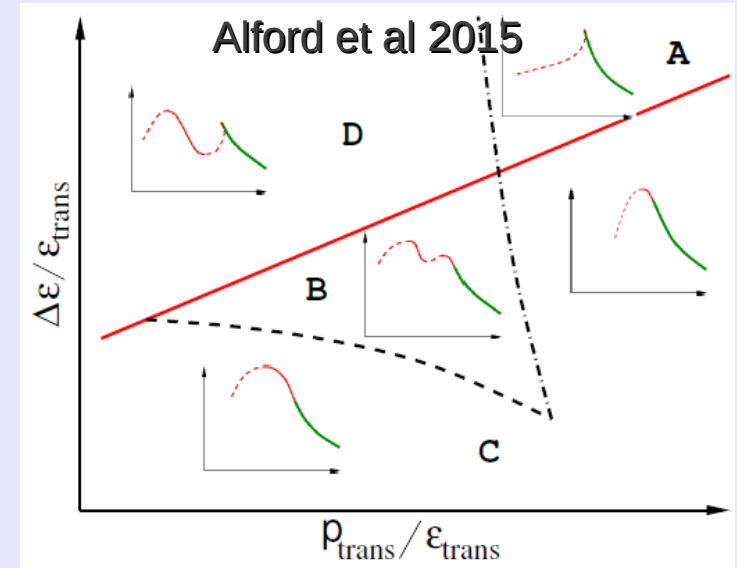
Simple parametrization of a first order phase transition to quark matter

$$\varepsilon(p) = \begin{cases} \varepsilon_{\text{NM}}(p) & p < p_{\text{trans}} \\ \varepsilon_{\text{NM}}(p_{\text{trans}}) + \Delta\varepsilon + c_{\text{QM}}^{-2}(p - p_{\text{trans}}) & p > p_{\text{trans}} \end{cases}$$

It is possible to construct $1.4M_{\text{sun}}$ hybrid stars solutions with radii as small as 11.5km.

Those solutions predict a very early onset of the phase transition to quark matter in beta stable nuclear matter.

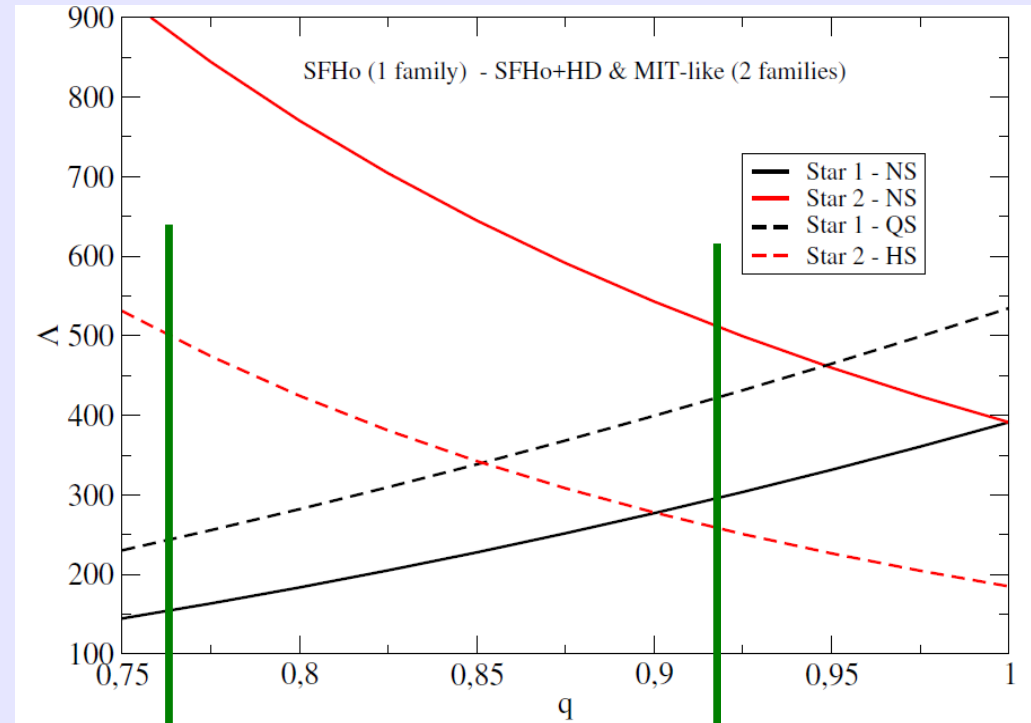
Hyperons are “eaten up” by quark matter.



Tidal deformability

Compute the deformability for the two stars of GW170817 at fixed total mass (i.e. $2.74M_{\text{sun}}$) and for various values of the mass ratios $q=M_2/M_1$

- 1) One family of neutron stars (SFHo model)
- 2) Mixed system: the most massive star is a quark star and the second star is a neutron star



Small asymmetry for 1family

Large asymmetry for 2families
Crossing point at $q < 1$

A mixed system would be highly asymmetric: more efficient for what concerns the mass ejected

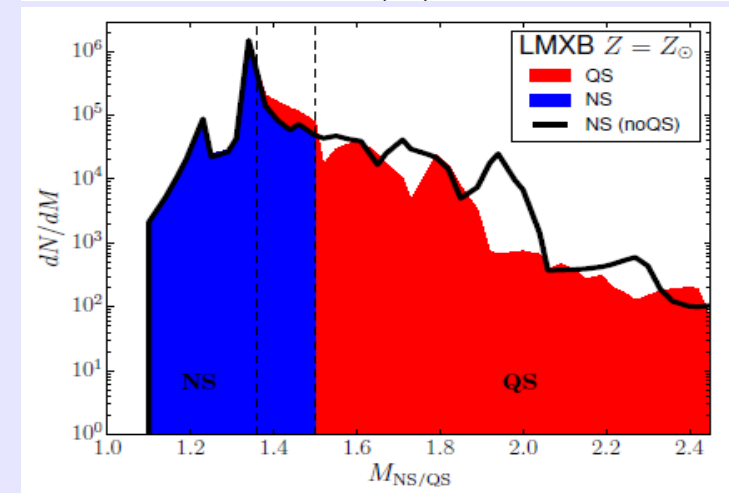
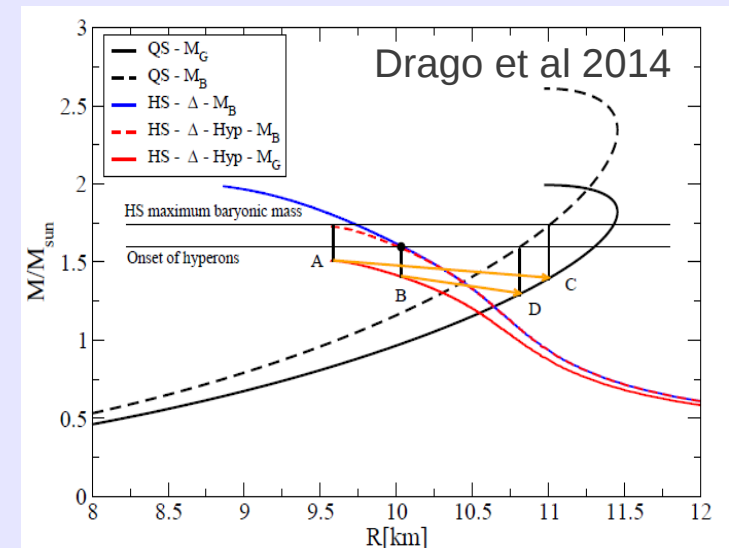
Strange star mergers from population synthesis

(Wiktorowicz et al 2017)
StarTrack code by Belczynski 2002

Simulation of 2 millions binaries with three different metallicities, statistical distributions of progenitor masses, binary separation, eccentricities and natal kicks.

Two families scenario: maximum mass of hadronic stars $1.5-1.6 M_{\text{sun}}$ Massive stars are strange stars.

A small modification of the mass distribution around $1.4 M_{\text{sun}}$



Evolution of two MS stars leading to a double strange star system.

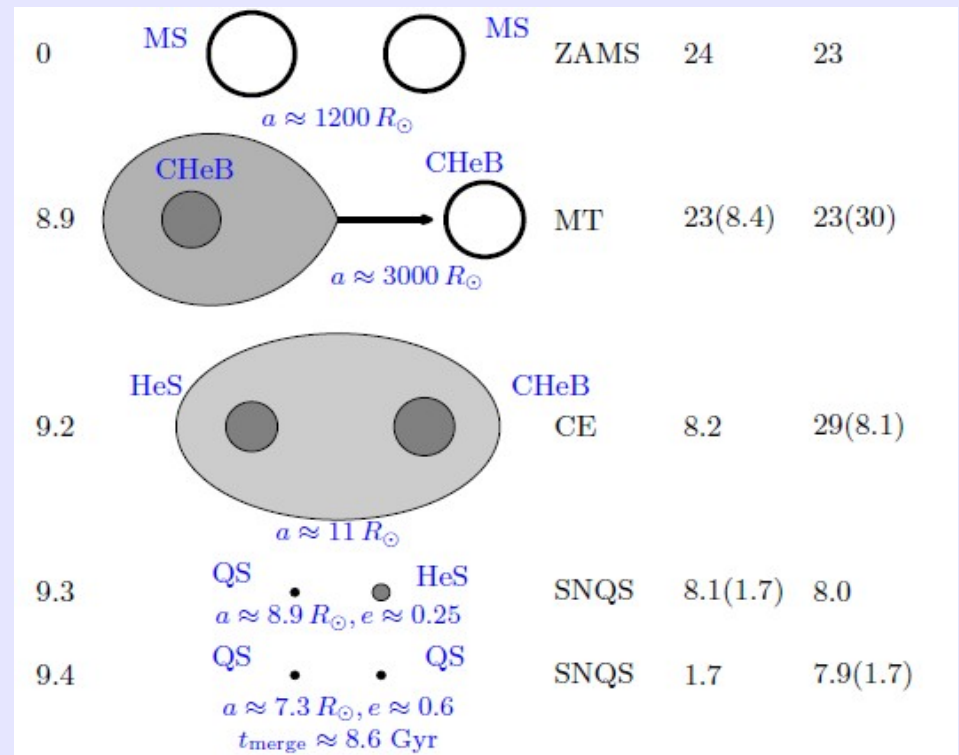


TABLE 1
NUMBER OF QS/NS IN BINARIES

Metallicity	#QS ^a	#NS ^a	f_{QS}^{b}	#NS(noQS) ^c	f_{cr}^{d}
		ALL			
Z_{\odot}	9.0×10^4	7.2×10^6	0.01	7.3×10^6	1.10
$Z_{\odot}/10$	2.7×10^5	7.4×10^6	0.04	7.7×10^6	1.37
$Z_{\odot}/100$	1.5×10^5	1.0×10^7	0.01	1.0×10^7	1.57
		LMXB			
Z_{\odot}	1.6×10^4	6.1×10^4	0.26	7.7×10^4	1.61
$Z_{\odot}/10$	1.2×10^4	1.5×10^5	0.08	1.6×10^5	1.22
$Z_{\odot}/100$	7.0×10^3	2.1×10^4	0.25	2.9×10^4	1.31
		DQS/DNS			
Z_{\odot}	–	6.4×10^5	–	6.6×10^5	0.88
$Z_{\odot}/10$	<u>4.2×10^3</u>	5.2×10^5	0.08	5.2×10^5	1.22
$Z_{\odot}/100$	–	7.6×10^5	–	7.6×10^5	0.86

NOTE. — QS and NS quantities per MWEG at present time for $M_{\text{max}}^H = 1.5 M_{\odot}$. ALL – all binaries; LMXB – mass-transferring binaries; DQS/DNS – double QS/NS.

^a Number of QS (#QS) and NS (#NS)

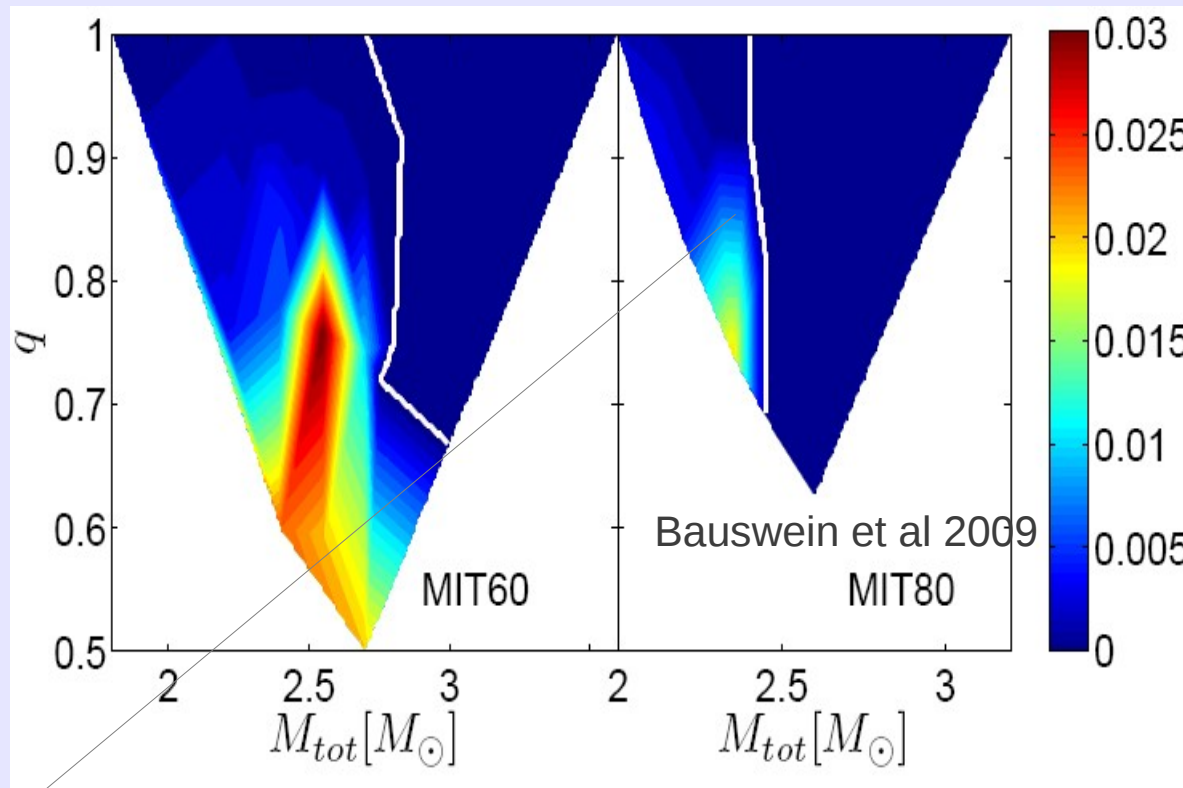
^b fraction of QSs; defined as $f_{\text{QS}} := \#QS / (\#QS + \#NS)$

^c number of NSs in the model without QSs (noQS)

^d change in a number of compact objects (QSs and NSs) in $1.36 - 1.5 M_{\odot}$ mass range; $f_{\text{cr}} := (\#QS' + \#NS') / \#NS'(\text{noQS})$ (mass range marked with ')

**Estimated rate of DQS mergers
(taking into account the
coalescence time): 10/Gyr per
MW galaxy**

Strange quark matter ejecta

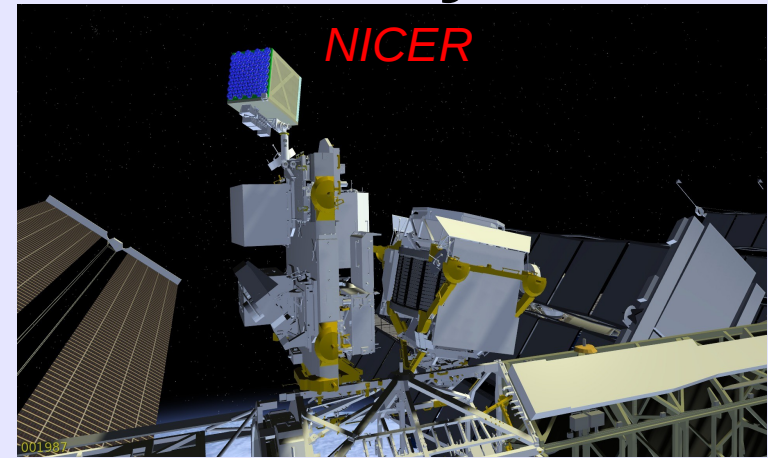


Prompt collapse: in those cases no matter ejected (limited by the numerical resolution $10^{-6} M_{\text{sun}}$). In the case of matter ejected, average mass $10^{-4} M_{\text{sun}}$.

To obtain an upper limit: take the typical value of NS mergers, $10^{-2} M_{\text{sun}}$, use the DQS merger rate: strange matter density in the galaxy $\rho_s = 10^{-35-36} \text{ g/cm}^3$. Important input for the searches of strangelets in cosmic rays (AMS02 - PAMELA)

Why is Neumatt very interesting: Upcoming measurements: X-rays

NICER (Neutron star Interior Composition Explorer) on the ISS, is collecting data since June 2017.



Temporal pulse profile of the hot spot will allow to measure the radius within 5% of error. Radii strongly depend on the adopted equation of state (see in the following). Possibility to test the models produced by Neumatt.

The closest and brightest millisecond pulsar

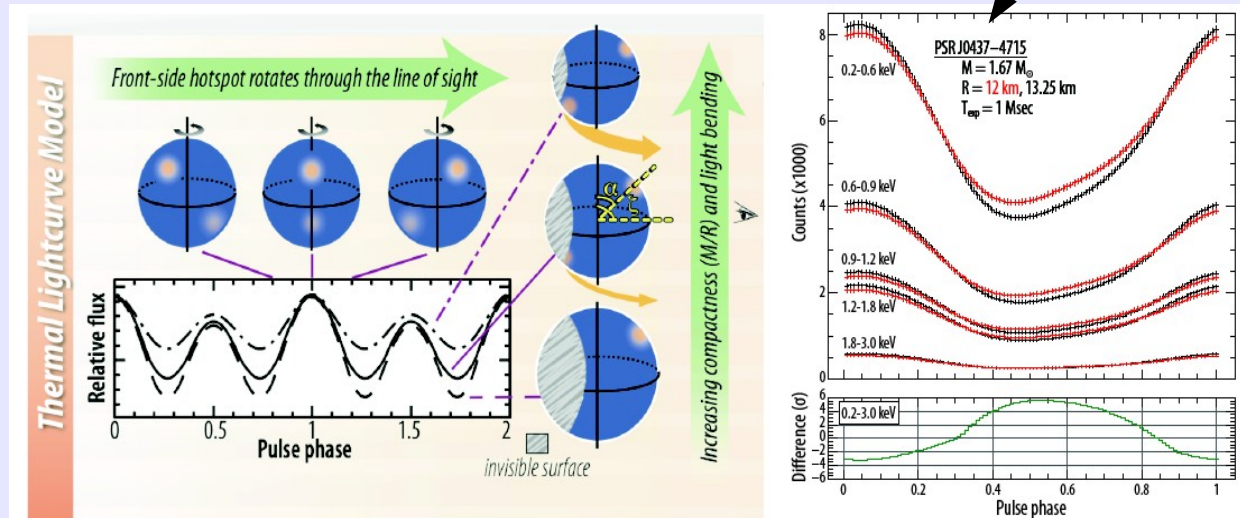


Figure 4. (Left) A distant observer sees X-ray intensity grow and fall as hot-spots on a neutron star surface spin through the line of sight. The far-side spot becomes more visible for smaller stars through gravitational light-bending, which depends on M/R ; thus, depth of modulation constrains compactness. (Right) Two sets of simulated NICER lightcurves, for stellar radii differing by $\pm 5\%$, show measurable differences in several energy bands for a 1 Msec exposure: $4-6\sigma$ differences per phase bin pinpoint the star's radius.

Upcoming measurements: radio

Square kilometer array.

Construction planned in 2018, data taking from 2020.

It will allow to discover 10^4 more pulsars, among which 100 in binaries \rightarrow 100 new mass measurements (masses higher than $2M_{\text{sun}}$?)

Possible to extract the momentum of inertia which together with a mass measurement will strongly constrain the equation of state. Test Neumatt calculations on rotating compact stars.



Gamma-ray-bursts events: SWIFT, FERMI in hard X-ray/soft gamma. Some GRBs may be generated by compact stars (magnetars). Some (indirect) info on the properties of matter already proposed (Gao et al. PRD 2016). Test Neumatt modeling of explosive phenomena.



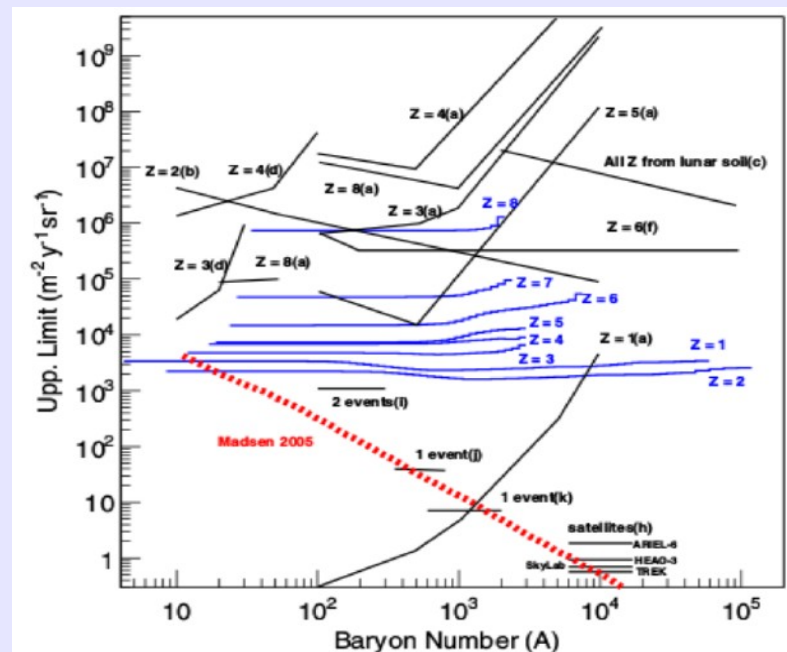
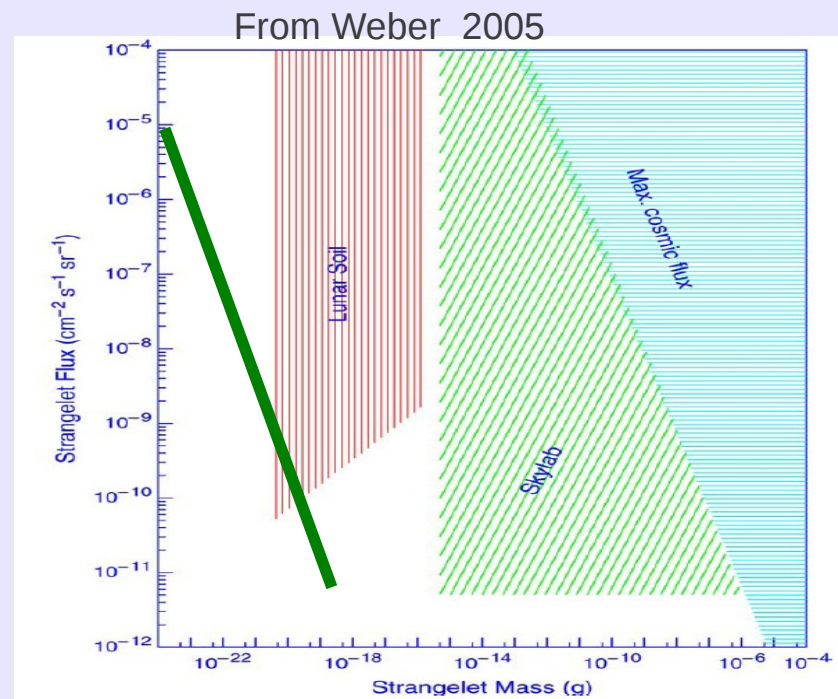
Flux of strangelets (with a specific value of mass number A , v : velocity of the galactic halo)

$$\frac{dj_s}{d\Omega} = \frac{\rho_s v}{4\pi A m_p}$$

$$dj_s/d\Omega \sim 10^{-5} \rho_{35}/A \text{ cm}^{-2} \text{ s}^{-1} \text{ sr}^{-1}$$

Considering the extreme upper limit on the mass ejected, our fluxes are compatible with the lunar soil searches.

Constraints from PAMELA: our upper limit violates the limits for $A < 10^3$... but the mass ejected is probably much smaller+difficult to fragment down to such small values of A (work in progress) (PAMELA coll. 2015)



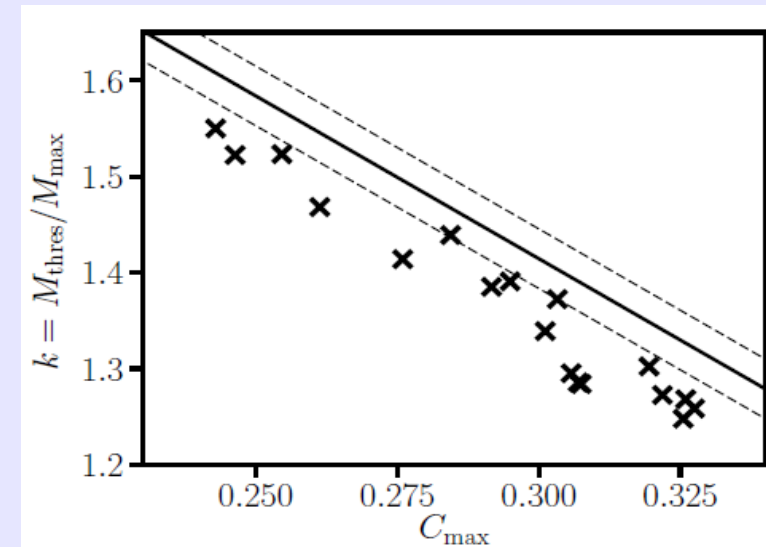
Prediction of the two families scenario on the fate of binary systems

Four possible outcomes (clearly distinguishable from the GWs signals):

- 1) Prompt collapse (large masses)
- 2) Hypermassive (intermediate masses) living ~ 10 ms
- 3) Supramassive stars (living $>$ few sec)
- 4) Stable stars

At fixed total mass, the outcome depends on the EoS. The mass above which a prompt collapse is obtained M_{thresh} is a simple function of M_{max} and its compactness.

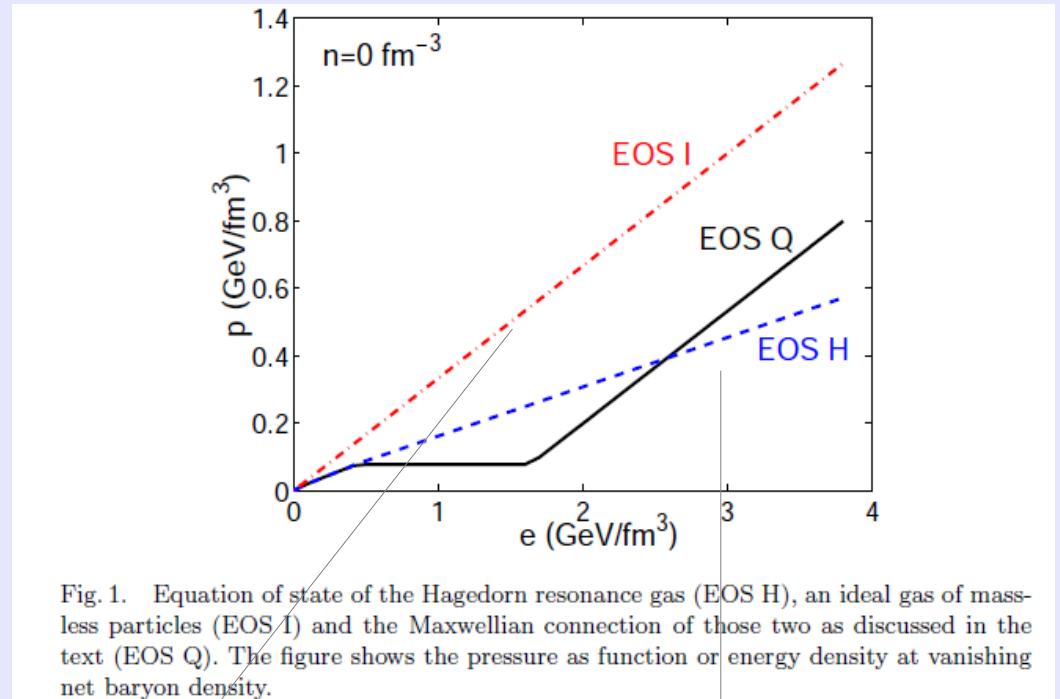
Bauswein Stergioulas 2017



... is this surprising?

Heavy ions physics: (Kolb & Heinz 2003)

Also at finite density the quark matter equation of state should be stiffer than the hadronic equation of state in which new particles are produced as the density increases



$p=e/3$ massless quarks

Hadron resonance gas $p=e/6$

Fragmentation

Work in progress

Condition to create a fragment: Weber number We larger than 1

$We = (\rho/\sigma) v_{\text{turb}}^2 d$ (mass density, surface tension, turbulent velocity and drop size). By assuming v_{turb}^2 to scale (Kolmogorov) with $v_0^2 (d/d_0)^{5/3}$ where $d_0 \sim 1\text{km}$ and $v_0 \sim 0.1c$, we obtain $d \sim 1\text{mm}$ and thus $A \sim 10^{39}$ **very big fragments**. There will be a further “reprocessing” via collisions, turbulence, evaporation ... very difficult problem!! There will be a distribution of mass number, with a minimum value which is probably much higher than 10^3 .

Depending on the size, different strangelets can act as seeds for the conversion of stars into strange stars (astrophysical argument against the Witten's hyp.).

Capture of strangelets by stars and conversion

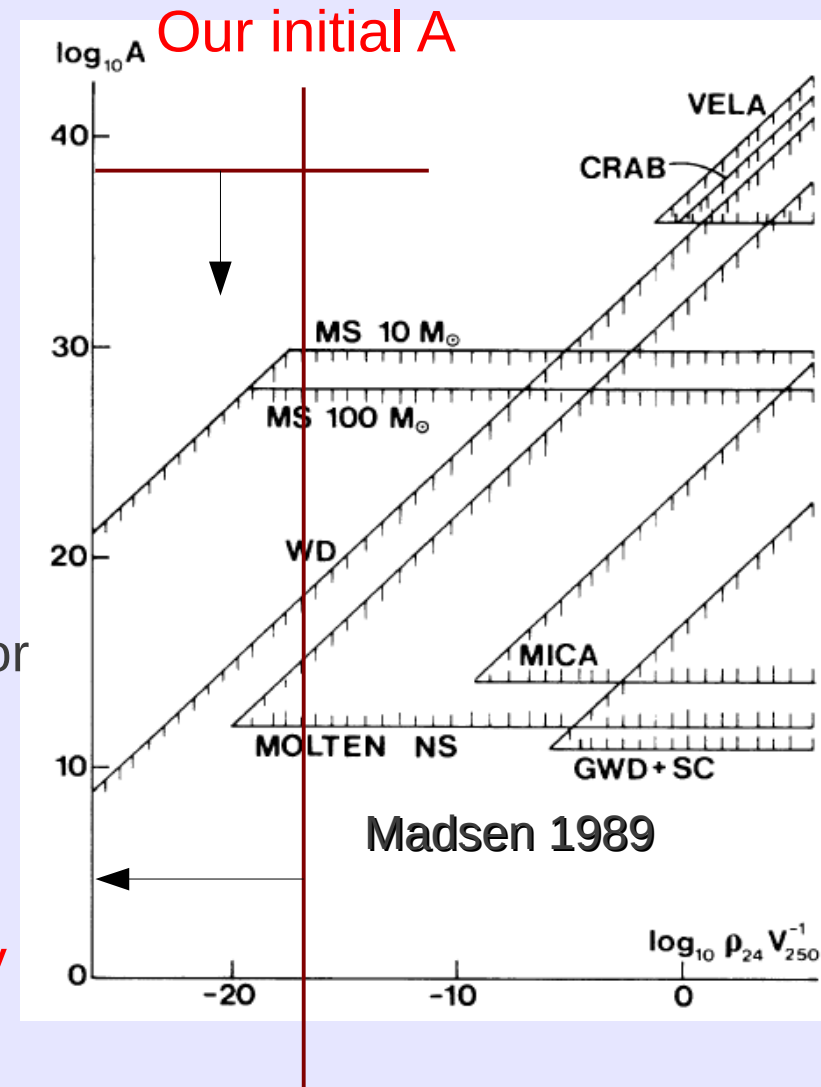
$$mv(x) \frac{dv(x)}{dx} = -\alpha \rho(x) v^2(x) + \frac{GM(x)m}{R^2(x)} - \epsilon(x)\alpha$$

Stopping force due elastic interaction with atoms

Interaction with the ion lattice

Main sequence stars: the most important limit. A strangelet can sit in the center of the star and “wait” for the core collapse SN and the neutronization. This would trigger the conversion of all protoneutron stars into strange stars.

- But:**
- 1) due to the 10 MeV temperature of the SN they could evaporate
 - 2) Not clear if fragmentation can work over ten orders of magnitude. Work in progress.



Our upper limit on the strange matter density

Two families and short/long GRBs

Internal X-ray plateau in short GRBs: Signature of supramassive fast-rotating quark stars?

Ang Li^{1,2*}, Bing Zhang^{2,3,4†}, Nai Bo Zhang⁵, He Gao⁶, Bin Qi⁵, Tong Liu^{1,2}

¹ Department of Astronomy, Xiamen University, Xiamen, Fujian 361005, China

² Department of Physics and Astronomy, University of Nevada Las Vegas, Nevada 89154, USA

³ Department of Astronomy, School of Physics, Peking University, Beijing 100871, China

⁴ Kavli Institute of Astronomy and Astrophysics, Peking University, Beijing 100871, China

⁵ Institute of Space Sciences, Shandong University, Weihai 264209, China

⁶ Department of Astronomy, Beijing Normal University, Beijing 100875, China

(Dated: June 10, 2016)

A supramassive, strongly-magnetized millisecond neutron star (NS) has been proposed to be the candidate central engine of at least some short gamma-ray bursts (sGRBs), based on the “internal plateau” commonly observed in the early X-ray afterglow. While a previous analysis shows a qualitative consistency between this suggestion and the Swift sGRB data, the distribution of observed break time t_b is much narrower than the distribution of the collapse time of supramassive NSs for the several NS equations-of-state (EoSs) investigated. In this paper, we study four recently-constructed “unified” NS EoSs (BCPM, BSk20, BSk21, Shen), as well as three developed strange quark star (QS) EoSs within the new confinement density-dependent mass (CDDM) model, labelled as CDDM, CDDM1, CDDM2. All the EoSs chosen here satisfy the recent observational constraints of the two massive pulsars whose masses are precisely measured. We construct sequences of rigidly rotating NS/QS configurations with increasing spinning frequency f , from non-rotating ($f = 0$) to the Keplerian frequency ($f = f_K$), and provide convenient analytical parametrizations of the results. Assuming that the cosmological NS-NS merger systems have the same mass distribution as the Galactic NS-NS systems, we demonstrate that all except the BCPM NS EoS can reproduce the current 22% supramassive NS/QS fraction constraint as derived from the sGRB data. We simultaneously simulate the observed quantities (the break time t_b , the break time luminosity L_b and the total energy in the electromagnetic channel E_{total}) of sGRBs, and find that while equally well reproducing other observational constraints, QS EoSs predict a much narrower t_b distribution than that of the NS EoSs, better matching the data. We therefore suggest that the post-merger product of NS-NS mergers might be fast-rotating supramassive QSs rather than NSs.

Within the proto-magnetar model of sGRBs, the formation of a quark star instead of a hadronic star in the merger would explain why the prompt phase of sGRBs is short (Drago, Lavagno, Metzger, Pagliara 2016)

Deconfinement and the protomagnetar model of long GRB

(Pili et al. 2016)

Conversion of rotating HSs

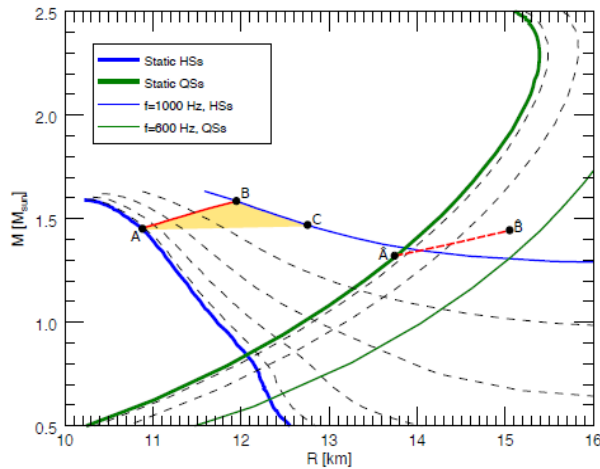


Figure 2. Gravitational mass as a function of the circumferential radius for both HSs and QSs. Thin dashed lines are sequences of stars at a fixed frequency from the non-rotating configurations (thick solid blue and green lines) to the configurations rotating at the maximum frequency (thin solid blue and green lines) and spaced by 200 Hz. The yellow region shows hadronic configurations centrifugally supported against deconfinement. Red lines and labels are the same as in figure 1.

Delayed deconfinement

Table 2. Spin-down timescales to start quark deconfinement Δt_{sd} together with the associated variation of the rotational kinetic energy ΔK_{sd} starting from an initial spin period P_i for the equilibrium sequences shown in figure 3. We also report the spin-down timescales Δt_q (defined as the time needed to half the rotational frequency of the QS) and the corresponding rotational energy loss ΔK_q after quark deconfinement. The initial magnetic field is of 10^{15} G.

M_0 [M_{\odot}]	$P_i \rightarrow P_d$ [ms]	Δt_{sd}	ΔK_{sd} [10^{52} erg]	Δt_q	ΔK_q [10^{52} erg]
1.666	1.0 \rightarrow ∞	∞	5.91	-	-
1.677	1.0 \rightarrow 3.3	2.7 hr	5.48	37 hr	0.19
	2.0 \rightarrow 3.3	1.8 hr	0.82		
	3.0 \rightarrow 3.3	37 min	0.13		
1.687	1.0 \rightarrow 2.5	1.5 hr	5.13	21 hr	0.33
	2.0 \rightarrow 2.5	36 min	0.46		
1.698	1.0 \rightarrow 2.0	55 min	4.68	14 hr	0.53
1.733	1.0 \rightarrow 1.4	23 min	3.37	8.2 hr	1.20
1.785	1.0 \rightarrow 1.1	6 min	1.37	5.4 hr	1.95
1.820	1.0 \rightarrow 1.0	0	0	4.6 hr	2.41

Many examples of “double bursts” in the LGRBs data

UNUSUAL CENTRAL ENGINE ACTIVITY IN THE DOUBLE BURST GRB 110709B

BIN-BIN ZHANG¹, DAVID N. BURROWS¹, BING ZHANG², PETER MÉSZÁROS^{1,3}, XIANG-YU WANG^{4,5}, GIULIA STRATTA^{6,7}, VALERIO D’ELIA^{6,7}, DMITRY FREDERIKS⁸, SERGEY GOLENETSKI⁸, JAY R. CUMMINGS^{9,10}, JAY P. NORRIS¹¹, ABRAHAM D. FALCONE¹, SCOTT D. BARTHELME¹², NEIL GEHRELS¹²

Draft version June 24, 2013

ABSTRACT

The double burst, GRB 110709B, triggered *Swift*/BAT twice at 21:32:39 UT and 21:43:45 UT, respectively, on 9 July 2011. This is the first time we observed a GRB with two BAT triggers. In this paper, we present simultaneous *Swift* and Konus-WIND observations of this unusual GRB and its afterglow. If the two events originated from the same physical progenitor, their different time-dependent spectral evolution suggests they must belong to different episodes of the central engine, which may be a magnetar-to-BH accretion system.

Subject headings: gamma-ray burst: general

